University of Puerto Rico
Rio Piedras Campus
Faculty of Natural Sciences
Department of Chemistry

# Design of responsive cellulose-block copolymer membranes for the remediation of organic emerging contaminants: A selective adsorption approach for electron-deficient aromatic compounds.

By
Jairo Herrera-Morales

August 2019

Accepted by the Faculty of Natural Sciences from University of Puerto Rico in Partial Fulfillment of Requirement to obtain the degree of Doctor in Philosophy

_____

Dr. Liz Diaz-Vazquez

Department Chair

_____

Dr. Eduardo Nicolau

Advisor

August 2019

## Table of Contents

## List of Figures

## List of Abbreviations and chemical formulas

| | |
|---|---|
| CECs | Contaminants of Emerging Concern |
| EOCs | Emerging Organic Contaminants |
| NC | Nano-Cellulose |
| Oxidized-NC | Oxidized Nano-Cellulose |
| CNC | Cellulose Nano-Crystals |
| PEG | Polyethylene Glycol |
| Jeffamine ED 600 | O,O′-Bis(2-aminopropyl) polypropylene glycol-block-polyethylene glycol-block-polypropylene glycol |
| NC-Jeffamine | Nano-Cellulose grafted with Jeffamine ED 600 |
| CNF | Cellulose Nano-Fibers |
| TEMPO | 2,2,6,6-Tetramethyl-1-piperidinyloxy |
| EDC | N-(3-Dimethylaminopropyl)-N′-ethylcarbodiimide |
| DFT | Density Functional Theory |
| VASP | Vienna Ab initio Simulation Package |
| DO | Degree of oxidation |
| DS | Degree of substitution |
| CTA | Cellulose Tri-Acetate |

| | |
|---|---|
| NaOCl | Sodium Hypochlorite |
| SMX | Sufamethoxazole |
| ACE | Acetaminophen |
| DEET | N,N-Diethyl-m-toluamide |
| SDZ | Sulfadiazine |
| OMZ | Omeprazole |
| AGU | Anhydroglucose Unit |
| BET | Brunauer-Emmett-Teller |
| BCP | Block-Copolymer |
| Sulfo-NHS | N-hydroxysulfosuccinimide Sodium salt |
| NMR | Nuclear magnetic resonance |
| P4VP-PEO | Poly(4-vinylpyridine-b-ethylene oxide) |
| TMPES | Trimethoxy(2-phenylsthyl)silne |
| CA | Contact Angle |
| RO | Reverse Osmosis |
| FO | Forward Osmosis |
| NIPS | Non-Solvent Induced Phase Separation |
| EDS | Energy dispersive spectroscopy |

| | |
|---|---|
| DMAc | N,N-Dimethylacetamide |
| DLS | Dynamic Light Scattering |
| AFM | Atomic Force Microscopy |
| EDA | Electro-donor acceptor |
| FTIR | Fourier Transformed Infrared |
| FTIR-ATR | Fourier Transformed Infrared - Attenuated Total Reflectance Spectroscopy |
| HCl | Hydrochloric acid |
| NaOH | Sodium Hydroxide |
| SEM | Scanning electron microscopy |
| TEM | Transmission electron microscopy |
| TGA | Thermogravimetric analysis |
| TMCS | Trimethylchlorosilane |
| XRD | X-ray diffraction |
| XPS | X-ray photoelectron spectroscopy |

## Abstract

Organic emerging contaminants (OECs) or contaminants of emerging concern (CECs) are molecules that were previously unaccounted for in terms of water quality standards and are known now to have adverse ecological and human health effects. The primary source of OECs includes, among others, active pharmaceutical ingredients and personal care products discarded to the environment through the regular municipal wastewater plants. These contaminants keep building up over time, mainly owing to the lack of cost-efficient technologies to remediate their presence in effluents. Among the different water filtration technologies, activated carbon (AC) is the choice of preference for the removal of EOCs due to its high adsorption capacity. Nevertheless, the adsorption efficiency of AC rapidly decreases due to organic fouling. Besides, the regeneration of AC is time-consuming and power-intensive; therefore, reuse of this material is somewhat limited. An alternative approach lies in water filtration using selective and reusable membranes. However, research in this area is still limited, and consequently, it is imperative to close the knowledge gap related to the rational design of membranes for the remediation of EOCs. Following that ideal, this research focused on the study and optimization of responsive membranes based on alternative materials, named, block copolymer (BCP)-cellulose conjugates. BCPs are polymers with a wide variety of molecular architectures based on the composition and molecular weight of its constituting monomers. This versatility allows BCPs to interact with organic contaminants through physical and chemical interactions selectively and reversibly that can be triggered by external stimulus. On the other hand, cellulose is an abundant, inexpensive, and renewable biopolymer that in this case is intended to provide structural support to the BCPs.

This thesis has been developed through three main objectives. Initially, it was evaluated the use of nanocellulose and polyethylene glycol-based BCP to prepare composites for sorption of EOCs. Experimental and theoretical results suggested that the material was able to adsorb EOCs via electrostatic interactions (H-bonds and Van der Waals). For the second objective, it was prepared low-cost, nanocellulose-BCP films modified with an alkoxysilane where the BCP, Poly(4-vinyl pyridine-b-ethylene oxide) (P4VP-PEO) was the active adsorption material. This BCP allowed the adsorption of sulfamethoxazole via electron donor-acceptor (EDA) interactions, which are selective and reversible, a key characteristic for the reuse of the films. In addition, the hydrophobic alkoxysilane, Tri-methoxy (2-phenyl ethyl)silane provided aqueous stability to the films against dispersion through several adsorption cycles. Finally, cellulose tri acetate-P4VP-PEO membranes were prepared and optimized using non-solvent induced phase separation (NIPS) method. These membranes presented high surface porosity with internal interconnected hierarchical pores containing P4VP-PEO for competitive adsorption of EOCs while allowing reusability. In this study was evaluated the adsorption selectivity of the membranes toward EOCs. Results suggested that higher electron-deficient aromatic EOCs translated to higher adsorption capacity of the membrane. Overall results of this study led into an efficient, low-cost, and eco-friendly method to produce selective and reusable adsorption membranes that contribute to further development of large-scale EOCs remediation applications.

Design of responsive cellulose-bock copolymer membranes for the remediation of organic emerging contaminants: A selective adsorption approach for electron-deficient aromatic compounds.

**Acknowledgements**

Firstly, I would like to express my sincere gratitude to my advisor, Dr. Eduardo Nicolau for the allowing me to be part of his team, for the continuous support, his motivation, and compromise with the laboratory. His leadership and guidance helped me to shape and accomplish this project.

I also thank my fellow lab mates for the stimulating discussions. It feels great to think about how we were growing our intellect and systematic thinking during all these years. Let`s not forget all the times that we share outside the laboratory setting, that is priceless. I also want to express my appreciation and love to my wife, Jeannette Cruz, for the support throughout the years: to you and my children, Jhair, Isabel, and Jairo Andrés, this is for you! You are the ultimate motivation to always pursuit for something better in our lives.

Special thanks to my undergraduate students, Kathleen Morales, Damarys Ramos, José Lasalde Ramírez, Laura Penabad, Jose Luis Ramírez, and Miguel Betancourt. I truly recognize that your help and support provided a solid base to this research.

I would also like to acknowledge the sources of financial support during my research work: NASA EPSCoR program under Grant Number NNX14AN18A, the Puerto Rico Science, Technology, and Research Trust and the Institute for Functional Nanomaterials. Also, I thank the Office of the Dean for Graduate Studies and Research (DEGI) for their initial financial support.

Finally, I would like to thank my family in Colombia: my parents, Jairo and Regina, my sisters Hilda and Patricia. I know that even from the distance, I will always have your support.

CHAPTER ONE

# 1. INTRODUCTION

## 1.1.Background

In order to meet water quality standards, investigators have focused the attention to the removal of nutrients, bacteria, viruses, heavy metals, and priority pollutants. The development and improvement of separation techniques have allowed for the detection of extremely low concentrations (µg/L-ng/L) of different contaminants in surface water [1, 2]. Indeed, the persistence of these contaminants in the environment has caused an increasing concern regarding the impact of such contaminants on the aquatic life and consequently the human health since their toxicity, behavior, and fate are not well understood. Hormones, human and veterinary pharmaceuticals, (including their metabolites), surfactants, X-ray contrast media, and pesticides are a few examples of the so-called contaminants of emerging concern (CECs) [3-5]. Wastewater from households, hospitals, construction sites, transportation, industrial-scale animal feeding operations, and manufacturing are considered as the principal sources of CECs [1, 6]. Amongst the CECs found in the environment, pharmaceutical and personal care products are the most prevalent. These contaminants are also known as emerging organic contaminants (EOCs) given their organic chemistry nature and are common in surface and groundwater. Efforts to improve the efficiency of water remediation toward these contaminants have been the subject of studies in recent years. These include nanofiltration, reverse osmosis [7], ultrafiltration, adsorption with activated carbon [8], degradation with microorganisms, and electrooxidation [9]. Commercial membranes for water purification have undergone promising improvements, allowing for low energy consumption. Nevertheless, still to these

days, these membranes are not cost-effective or fully effective in removing EOCs. These difficulties derive from expensive preparation methods and source materials, as well as the lack of reactive surface functionalities [10].

Thus, in this work we have focused our attention on the development of membranes for the adsorption of EOCs based on selective interactions between these contaminants and specific functionalities introduced on the membrane structure. These functionalities are presented as block copolymers (BCPs) embedded in eco-friendly supports base of cellulose and cellulose derivatives. The study proposes the preparation of membranes through inexpensive phase separation methods that would allow the configuration of surface and pores homogeneity and enhanced adsorption efficiency of the membrane.

Surface and structural modification with appropriate functionalities, absorbents-EOCs contact interface, and adsorption reversibility (adsorbent reusability) are the key concepts in the design of the membrane. Optimization of those parameters allowed us to contribute to the field of water remediations of EOCs and to open the door for the development of large-scale approaches.

### 1.2.Statement of the problem

EOCs are known to be more frequently present in aquatic ecosystems due to the wide variety of waste source that reach water effluents [11]. Although in principle, wastewater treatment plants may remove these contaminants, this is not always the case. Wastewater treatment plants typically employ processes of flocculation-filtration as well as oxidation-chlorination. However, flocculation-filtration methods are not able to completely remove EOCs due to the low concentration of the contaminants and ineffective physical interaction.

Application of oxidation processes such as chlorination, ozonation or even UV photolysis, has showed, in most cases, effective degradation of EOCs. Nonetheless, these processes do not account as actual removal methods, and the byproducts that are created after these processes such as organochlorine specie can be more toxic than the initial compounds [12-16]. Currently, the adsorption of EOCs with activated carbon is a preferred method because of the material`s high porosity (surface area), which allows for effective adsorption of the contaminants [5, 17]. However, the production of activated carbon demands considerable amounts of energy and activated carbon pores can easily undergo fouling, drastically reducing its adsorption efficiency [18, 19]. Among other strategies used to remove EOCs from wastewater and drinking water, processes that involve the use of membranes are considered quite promising [20]. Membrane processes such as forward osmosis (FO) and reverse osmosis (RO) have been extensively studied for the rejection of EOCs. However, these methods still rely on physical rejection, meaning that there is no selectivity, and organic fouling is still an issue [21-26].

Despite the advances in polymer synthesis and membrane production technologies, insufficient or no research has been performed to tackle the water remediation of EOCs. This is a consequence of the lack of selectivity and poor cost-effectiveness of polymers used in commercial purification membranes. We hypothesize that porous adsorption membranes are a feasible strategy to overcome the deficiencies of those common methods. Adsorption can be controlled by the addition of specific functionalities to polymeric rearrangement producing high porosity. These functionalities can also allow the reusability of the membranes by reversible adsorption as a response to external stimuli. This is where block copolymers fill the gap. BCP introduce a wide variety of covalently linked

functionalities while allowing superior control over membranes features such as pore homogeneity, hydrophilicity, and mechanical properties, among others. These enhanced properties are possible because BCP can be configured into a nearly infinite number of molecular architectures based on the composition and molecular weight of its constituting monomers [27-29]. In order to increase the commercial potential of block copolymer membranes, it is pertinent to provide structural support. We can achieve this by the incorporation of reinforcement materials such as cellulose and cellulose derivatives. These biopolymers are obtained from naturally occurring sources, are inexpensive, biodegradable, and practically renewable. These characteristics make them sustainable and environmentally friendly materials for the intended application.

This research addressed the evaluation of cellulose materials modified by block copolymers as competitive candidates for the preparation of membranes for the selective adsorption of EOCs. Results are intended to improve the understanding of cellulose-BCP composite, membrane preparation methods, and EOC-adsorbent interaction.

### 1.3.Research Objectives

To accomplish the examination and preparation of responsive and selective membranes for the adsorption of EOCs, three objectives were proposed: evaluation of the starting materials, applications, and development of the porous membranes.

#### 1.3.1. Objective 1. Evaluation of cellulose-BCP composites for the sorption of EOCs

A comprehensive analysis of the starting materials and their evaluation as feasible adsorbents for EOCs was performed. The first aim of this study was intended to prepare

composites composed by a BCP chemically attached to crystalline cellulose particles. These particles were used to form a suspension in water to better interact with the EOCs.

**Specific Aim:** Nano-Cellulose surface was modified to form carboxylic acids to later react with an aminated BCP through the formation of amide bonds. The resulting particles were placed in contact with SMX, ACE, and DEET to evaluate their adsorption capacity using experimental methods and theoretical methods.

### 1.3.2. Objective 2. Reusable nanocellulose-block copolymer films for the removal of OECs

Preparation of nano-cellulose composites and the adsorption evaluation towards EOCs was completed. However, adsorption evaluation was challenging to execute since the particles were difficult to recover from the solution using conventional methods. Ultrafiltration was required to separate the particles from the aqueous solution, and the material was almost impossible to reuse. In addition, the adsorption capacity of material should be improved. A new strategy involving the preparation of cellulose nano-fibers (CNFs) films modified by a hydrophobic additive and a new BCP was carried out. The intention was to avoid the dispersion of the material in the aqueous solution, allowing controlled adsorptions, easy recovery of the films, and reusability.

**Specific Aim:** CNFs were modified with the alkoxysilane, TMPES and the BCP, P4VP-PEO to later prepared films by a simple vacuum filtration method. The films were characterized, and the stability in water was evaluated. Films were then placed in contact with SMX as EOC model to test their adsorption capacity and reusability.

### 1.3.3. Objective 3. Preparation of porous cellulose tri-acetate membranes with an adsorption active polymer for remediation of EOCs

As the incorporation of the new BCP, P4VP-PEO proved to be successful for the adsorption of SMX; the next step was to evaluate their selectivity toward other EOCs. In the meantime, it was determined that the films prepared in the previous experiment could beneficiate with and increased porosity. Nevertheless, the vacuum filtration method only allows the accumulation of fibers, meaning there was little margin for improvement. To overcome that issue, it was decided to produced membranes using non-solvent induced phase separation. For that, the polymeric support was provided by cellulose tri-acetate (CTA) reinforced with a polyester mesh. P4VP-PEO embedded in the CTA polymeric structure.

**Specific aim:** CTA and P4VP-PE were dissolved in acetone/DMAc to be cast in a polyester mesh. After NIPS, the resulting porous membranes were characterized and tested for the absorption of EOCs, SMX, OMZ, and SDZ. The adsorption capacity evaluation was executed by kinetic and isotherm models taking into consideration the selectivity of the membrane. Reusability tests were executed for all EOCs.

The following chapters will elaborate on the details of this research, from the literature review, through the methodology. In the successive chapters all the findings will be discussed.

CHAPTER 2

# 2. LITERATURE REVIEW

## 2.1 Emerging organic contaminants

The increasing diversity of organic compounds, most of them synthetic, that the human society uses for a wide range of purposes has generated many questions regarding their occurrence and fate in the environment. The consequences of the contamination of surface and groundwater resources with these synthetic organic compounds, despite being a concern, are not well understood. Particularly, synthetic organic contaminants that were unaccounted before are now being detected in the environment due to the advent of improved analytical methods [30-32]. These contaminants are now referred as organic emerging contaminant (EOCs), and include synthetic materials produced by pharmaceuticals, personal care products, pesticides, industrial compounds, as well as by-products, nano-materials, food additives, among others [3, 33]. This issue is now out of proportion given the increasing human population and insufficient regulatory practices for acceptance criteria of wastewater, and more critical, water for consumption. It is of concerns that these contaminants pose a serious risk to aquatic life and human health, as most of them are considered disruptors of the endocrine system [34]. Endocrine disruptors are compounds that disturb the endocrine system by mimicking or blocking the normal function of hormones [35-37]. Additionally, these compounds have negative effects at very low concentration, which implies that trace or even ultra-trace concentrations of EOCs pose adverse effects in aquatic biota and therefore, human health [38]. In most cases, EOCs are ingested via food/drink intake, which leads to bioaccumulation and biomagnification throughout the food chain. This phenomenon can be seen, for example, in fish-eating

animals that regularly contain higher concentrations of EOCs than those found in fish on which they feed [39]. In that order of ideas, a similar effect could be found in humans since fish is part of the diet of most the modern society.

By exploring the extension of the EOCs distribution among different environment, it was noted that the case of Puerto Rico is not an exception. A study conducted by the Puerto Rico Environmental Quality Board (PREQB) and reported in 2013 revealed that at least one or more of the EOCs reported in the literature were detected at trace concentration (less than 1 ppm) in 80% of the water sources analyzed [40]. This is of extreme concern given the limited available water sources in the island and consequently the increased related health problems that it may impose to the exposed communities. Therefore, it is pertinent to address the remediation of water sources using the appropriated techniques in benefit of the environment and human integrity.

## 2.2 EOCs Remediation techniques

### 2.2.1 Conventional methods

Wastewater treatment plants are characterized for the employment of conventional methods such as flocculation/coagulation followed by oxidation for the remediation of contaminants. Flocculation and coagulation methods use materials intended to form aggregates in the aqueous solution, and in the process capture the contaminants. Once the aggregates are large enough, they can be removed from the surface of the water tanks. These are used as initial remediation steps since they are unable to remove most of the contaminants present in the solution. This limitation is related to the type of material used as flocculant. In general, flocculants can capture only ionic species, namely positively or

negatively charged compounds. Although EOCs can be presented as charged species in aqueous solution, most of them are neutral aromatic compounds that do not interact with the flocculant [41]. For that reason, flocculation/coagulation need to be complemented by other methods such as micro-oxidation or chemical oxidation. The use of microorganism for the degradation of EOCs can be performed in bioreactors, were bacteria use the contaminants as a carbon source. However, most of EOCs cannot be degrade by bacteria, and mostly bioaccumulates into the system [42]. Oxidation processes are generally achieved using chlorination, ozonation, or photolysis. Even to these days, chlorination is still the conventional method of preference for disinfecting drinking water. Disinfection occurs due to the strong oxidation power of chlorine that degrades the contaminant. However, the oxidation capability of chlorine is highly affected depending on the functionalities of the benzene ring of the EOCs [43]. This limitation translates to the formation of chlorinated species that are widely known for their toxicity. Similar results can be obtained when ozonation or photolysis is used to degrade EOCs [44]. As a general consideration regarding WWTPs using conventional methods suggests that they are ineffective removing EOCs, meaning that a considerable number of those contaminants remains in the solution.

### 2.2.2 Activated carbon

Perhaps, activated carbon (AC) is the most recognizable material for the adsorption of contaminants. In fact, this material is even used for the adsorption of small gas molecules due to the large number of nano- and micro-pores that composed its structure [45]. In terms of the adsorption of EOCs, several studies have demonstrated the enormous capability of AC as a remediation material [46-49]. Although there is controversy regarding the

adsorption mechanism of AC with emerging contaminants, there is some agreement in terms of the π interactions. One of those approaches involves the formation of π donor-acceptor complexes between the aromatic ring of contaminants and graphene planes of AC. It is also considered the formation of donor-acceptor complexes with carbonyl functionalities of AC [50]. In addition to the excellent adsorption capabilities toward EOCs, AC is cost-effective as it can be prepared from almost any polymeric carbon material including carbon waste. However, this process cannot be considered eco-friendly since it requires high power outputs for the carbonization [51]. Additionally, the activation of AC generates considerable neutralization wastes that most of the time are difficult to dispose [52]. It is important to mention that AC can be used for adsorption until its active site are depleted, once that occurs, it is necessary to regenerate the AC structure. Since AC is an amorphous material, the regeneration process is complex, and it is generally achieved by pyrolysis, that once again requires high energy [53]. Putting aside the disadvantages of production of AC, *the adsorption characteristic and mechanism conferred by its chemical functionalities could be the key for the development of competitive and reusable materials.* This concept relies on the modification of support materials with functionalities that promote the adsorption of EOCs through electron-donor acceptor interactions, and at the same time allows a facile desorption process. This approach has been continuously addressed and will be discussed in the successive sections.

### 2.2.3 Membrane methods

As stated above, WWTPs employ conventional treatment processes that are ineffective in removing EOCs from wastewater. On the other hand, membrane processes such as forward osmosis (FO), reverse osmosis (RO), nanofiltration (NF), and ultrafiltration (UF),

have been successfully used for the rejection of EOCs [54-57]. FO is capable of produce high-quality permeate due to a high removal of various EOCs and the ability to operate under an osmotic driving force without requiring a hydraulic pressure difference [54]. In the case of RO, *rejection process involves the adsorption of the EOCs onto the membrane surfaces, followed by their dissolution into the membrane, and mass transport via diffusion into the membrane matrix* [58]. NF depends on several factors including the physicochemical properties of the EOCs that at the same time are affected by pH. UF membranes are generally affected by the EOCs size, hydrophobicity, and net charge. Even though studies have been addressing the membrane-contaminant interactions [58], *still there are knowledge gaps that need to be filled. It is where the implementation of materials that combines the adsorption characteristics of AC and the versatility of membranes justifies our research.*

### 2.2.4 Alternative methods

Remediation of EOCs could be highly benefited by introduction of novel materials based on supports matrices modified with moieties that allow selective adsorption of EOCs. For example, Bikash *et al.* developed high efficiency silica coated with a polymeric β-cyclodextrin for the adsorption of EOCs. Adsorption capacity of the materials were evaluated for 17-estradiol, PFOA, and bisphenol A solutions obtaining efficiencies higher than 90% for the three EOCs. The proposed adsorption mechanism suggested the formation of a complex between the cyclodextrin and the EOC involving two steps where the EOC enter the cyclodextrin cavity followed be the formation of hydrogen bonds [59]. This approach has been employed by Kawano *et al.* [60] as well as Qin *et al*. [61], suggesting a similar adsorption mechanism. Nanomaterials have been considered as other alternatives

for the adsorption of EOCs. Patino *et al.* performed adsorption experiment of several EOCs using modified multiwall carbon nanotubes (MWCNTs) with oxygen and nitrogen functionalities (carboxylic and amines, respectively). 1,8-dichlorooctane, nalidixic acid and 2-(4-methylphenoxy)ethanol were used as model EOCs, obtaining mixed adsorption capacities. Adsorption models and thermodynamics suggested a heterogeneous distribution of the adsorption sites, as well as Van de Waals forces as the predominant interactions [62].

**Block copolymers**. The use of novel materials has been justified in terms of the adsorption capabilities, but somewhat is still limited to modification with simple molecules. Still, there is a wide variety of complex molecules that could provide different characteristics to the adsorbent, and more interesting, switchable features as response to external stimulus. That is the case of block copolymers BCPs. BCPs introduce a wide variety of covalently linked functionalities while allowing superior control over membranes features such as pore homogeneity, hydrophilicity, and mechanical properties, among others. These enhanced properties are possible because BCP can be configured into a nearly infinite number of molecular architectures based on the composition and molecular weight of its constituting monomers [27-29]. BCPs can be fabricated from hydrophobic and hydrophilic monomers, that allows the variation of their conformation in response to external stimulus such as pH, solvent, temperature, etc. [63]. This characteristic has been exploited in the field of drug delivery [64, 65] and fabrication of iso-porous membranes [66]. Among the methods for the preparation of membranes, non-induced phase separation (NIPS) is commonly used. NIPS membranes can be produced from almost any polymer that can match the following conditions: be solubilized by an appropriate solvent or mixture of solvents and, be precipitated (coagulated) from a solution in continuous phase [66-68].

Hörenz *et al.* prepared asymmetric porous membranes via non-solvent induced phase separation using amphiphilic diblock terpolymers consisting of poly(styrene-co-isoprene) block and poly(N, N-dimethylaminoethyl methacrylate). It was observed the formation of integral asymmetric membranes structures with a minimum molar mass of 40 kD and enhanced membrane stability and morphologies at higher masses [69]. Vriezekolk *et al*. prepared different membranes using self-assembling polystyrene block poly(4-vinyl pyridine) with the idea of improving the efficiency of membrane production by phase inversion. The evaporation times were improved using the volatile solvent THF and non-volatile NMP at various ratios. Additionally, the performance of the resulting membranes was evaluated against the rejection of 10 nm Ag particles. Symmetric porous membranes were obtained when only NMP is employed, and then membranes with cylindrical micelles with a network of interconnected cylinders when using THF/NMP mixtures was achieved. This research suggests that the best structures and therefore best performance are obtained when 18 wt% of the polymer in a 70/30 THF/NMP ratio is used [70]. In order to increase the commercial potential of block copolymer membranes, it is pertinent to improve their mechanical properties, such as tensile strength. We can achieve this by the incorporation of BCPs to reinforcement materials. **Cellulose and cellulose derivatives** are a promising alternative for this task. These materials can be extracted from natural sources by acid treatment and depending on the extent of the reaction, the resulting structure can vary. For example, to remove its amorphous domains and obtain nano-cellulose (NC) structures such as cellulose nanocrystals CNC or cellulose nanofibers CNF [71-73]. NC primarily obtained from naturally occurring cellulose sources are inexpensive, biodegradable and practically renewable. that characteristics make them sustainable and environmentally friendly

materials for several applications. NC have been used as a nanosized reinforcement material given its Young's modulus range of 100 – 130 GPa [71]. There are several reports related to the significant increases in the tensile strength of polymer membranes when nanocellulose was to reinforce the structure [71, 74-76]. *In addition, NC surface have a high amount of hydroxyl groups that can be chemically modified to promote the covalent attachment of different functionalities* [77].

Despite the advances in polymer synthesis and membrane production technologies, there is still room for improvement. Taking advantage of the self-assembling properties of the BCP with functionalities such as pyridinium, highly selective membranes against EOC will be achieved. We are certain that this approach is reasonable due to the EDA interactions that are likely to occur between the phenyl rings of electron-deficient EOCs and pyridinium groups from the BCP through π-π interactions. Moreover, these interactions are reversible, which can allow the reusability of the materials. The knowledge acquired with this research will provide the basis to use cellulose-block copolymer composites as a material for the design of affordable water reclamation systems. It is expected that the positive repercussion on the field of water purification will be significant.

CHAPTER THREE

# 3. EXPERIMENTAL SECTION

## 3.1.Materials

### 3.1.1. Solvents

a. DMAc (N,N – Dimethylacetamide) ≥99% (Sigma Aldrich)

b. Acetone, ≥ 99.9% (Sigma Aldrich)

c. Ethanol, 190 proof (Pharmco)

d. Methanol, ≥ 99.9% (Sigma Aldrich)

### 3.1.2. Acids

a. Glacial acetic acid, ≥ 99.7% (Sigma Aldrich)

b. Hydrochloric acid, 36.5-38.0% (Fisher Scientific)

### 3.1.3. Reagents

a. Cellulose nano-crystals, 11.8 wt. % aqueous slurry (Process Development Center of the University of Maine)

b. Cellulose nano-fibers, 3 wt. % aqueous slurry (Process Development Center of the University of Maine)

c. Cellulose triacetate (39.8 wt. % acetyl, Mn ~ 30,000) (Sigma Aldrich)

d. TEMPO (2,2,6,6-Tetramethyl-1-piperidinyloxy), 98% (Sigma Aldrich)

e. TMPES (trimethoxy(2-phenylsthyl)silne), 98% (Sigma Aldrich)

f. Sodium hypochlorite, available chlorine 10-15% (Sigma Aldrich)

g. Sodium hydroxide, 99.99% (Sigma Aldrich)

h. Sodium bromide, 99.99% (Sigma Aldrich)

i. P4VP-PEO (poly(4-vinylpyridine-b-ethylene oxide) (20 kD-5 kD) (Polymer Source. Inc)

j. Jeffamine ED 600, (O,O′-Bis(2-aminopropyl) polypropylene glycol-block-polyethylene glycol-block-polypropylene glycol), 600 MW, 30 meq $NH_2$/g (Sigma Aldrich)

k. EDC (N-(3-Dimethylaminopropyl)-N′-ethylcarbodiimide), 98% (Sigma Aldrich)

l. Sulfo-NHS (N-Hydroxysulfosuccinimide sodium salt), 98% (Sigma Aldrich)

m. Sulfamethoxazole, analytical standard (Sigma Aldrich)

n. Acetaminophen, analytical standard (Sigma Aldrich)

o. DEET, analytical standard (Sigma Aldrich)

p. Omeprazole, analytical standard (Sigma Aldrich)

q. Sulfadiazine, analytical standard (Sigma Aldrich)

### 3.1.4. Gases

a. Helium high purity, 99.995% (Linde Gas)

b. Nitrogen high purity, 99.995% (Linde Gas)

### 3.1.5. Instrumentation

*3.1.5.1.General Instrumentation*

a. Balance, Ohaus AV64

b. Centrifuge, Thermo Scientific Sorvall WX+

c. Ultrasonic bath, MTI EQ-VGT

d. Oven, MTI Vacuum oven DZF-6020

e. Orbital Shaker – Brunswick Shaker Incubator Series 2000

f. Heater and Magnetic Stirrer, Corning PC-420D

g. Micrometer adjustable film applicator, MTI EQ-KTQ-100

*3.1.5.2.Specialized Instrumentation*

a. Agilent 1100 Series VWD HPLC quipped with a Hypersil BDS C18 column (150 x 4.6 mm, 5 µm)

b. Dynamic Light Scattering and Z-potential – Malvern Zetasizer Noano series

c. Thermogravimetric Analyzer – Perkin-Elmer STA 6000 simultaneous TGA

d. Fourier Transformed Infrared - Attenuated Total Reflectance Spectrophotometer – Bruker Tensor 27

e. Surface Area Analyzer Tristar II 3020

f. UV-Vis spectrophotometer – Thermo Genesys 10

g. UV-Vis spectrophotometer – Shimadzu UV-1800

h. Scanning Electron Microscope – JEOL JSM 6480LV

i. Atomic Force Microscope – Bruker Dimension Edge

j. Drop shape analyzer – Krüss DSA25S

k. X-ray photoelectron spectrometer – PHI 5600 equipped with an Al Kα mono and polychromatic X-ray source operating at 15 kV, 350 W with a pass energy of 58.70 eV.

l. Energy Dispersive Spectroscopy – EDAX PV7757/81ME

m. Conductivity Meter – Accumet Basic AB30

## 3.2. Experimental Procedures

### 3.2.1. Objective 1. Evaluation of cellulose-BCP composites for the sorption of EOCs

*3.2.1.1.TEMPO-mediated oxidation of NC*

Carboxylation of NC surface via TEMPO-mediated oxidation is a well-known method reported elsewhere [78-80]. First, we suspended NC (1.02 g, 6.3 mmol Anhydroglucose units, AGU), NaBr (324 mg, 3.15 mmol) and TEMPO (29.5 mg, 0.19 mmol) in 50 mL of deionized water under continuous magnetic stirring. The reaction was initiated by adding 0.94 mL of 12 wt. % NaOCl dropwise to the suspension for a molar ratio of 0.3 NaOCl/AGU. The pH was maintained at 10 using NaOH 0.5 M until no fluctuations were observed. At this point, 10 mL of methanol were added to halt the reaction, and the pH was lowered to 7 using HCl 0.5 M. The resulting suspension was dialyzed in a 3.5 kD membrane against deionized water at 4 ºC for 48 h to eliminate excess reagents.

*3.2.1.2.Polymer coupling onto NC surface by EDC/sulfo-NHS*

The surface of carboxylated polysaccharides can be easily modified with amine-terminated compounds via the formation of peptide bonds mediated by an EDC/sulfo-NHS coupling reaction [81, 82]. EDC (110 mg, 5.77 mmol) and sulfo-NHS (121 mg, 5.57 mmol) were dissolved in a 100 mL suspension of dialyzed oxidized NC. Amine-terminal Jeffamine ED 600 (184 mg, 5.52 meq of $NH_2$) was added to the suspension with respect to the carboxylic content of oxidized NC (determined by conductometric titration), pH was set to 8, and the reaction was left for 24 h at room temperature. Afterwards, the pH was lowered to acidity, and the suspension was dialyzed for 72 h in deionized water. To obtain

solid samples of the modified NC (NC-Jeffamine), suspensions were freeze-dried until complete dehydration.

*3.2.1.3.Characterization of NC grafted with block copolymer*

Fourier transform infrared (FTIR) spectra were recorded using attenuated total reflectance mode (ATR). The spectral width ranged from 400-4000 $cm^{-1}$, with a resolution of 4 $cm^{-1}$, an accumulation of 32 scans. TGA was used for thermal analysis. All the samples were heated from 30-750 ºC with a ramp of 20 ºC/min in an air atmosphere. DLS and Z-potential analysis was used to determine the average diameter and surface charge, respectively. All the samples were analyzed as aqueous suspension (~ 0.1 wt. %) at pH 7. SEM and AFM were used to record the micrograph of NC and modified NC. Samples for SEM analysis were suspended in deionized water, and then a drop was placed onto a carbon coated copper grid under air atmosphere until dryness. In the case of AFM, a diluted solution of the sample was spin-coated at 3,000 rpm for 20 s in a Silicon substrate (1-10 Ωcm). A surface area analyzer was used to determine the specific surface area of the samples applying the Brunauer-Emmett-Teller (BET) method. The degassing temperature was set at 120 ºC for 8 h under $N_2$ flow.

*3.2.1.4.Determination of block copolymer content on NC surface.*

Conductometric titration was used to determine the content of carboxylic acid groups on the surface of NC after the oxidation and the coupling reactions. A conductivity meter was utilized to monitor the titration of NC samples with an excess of 0.01 M HCl using 0.01 M NaOH as the titrant. The resulting plots showed the volume of NaOH necessary to determine the degree of oxidation (DO) using the following equation [83],

$$DO = \frac{162(C)(V_2 - V_1)}{w - 36(C)(V_2 - V_1)} \quad (1)$$

where $C$ is the concentration of NaOH (mol/L), $V_2$ and $V_1$ are volumes of NaOH (L), $w$ is the sample weight (g). Since the coupling reaction modifies the carboxylic acid into amide functional group, we can indirectly determine the block copolymer content in the surface of NC by subtracting DO before and after the EDC/sulfo-NHS reaction.

*3.2.1.5.Batch adsorption experiments of contaminants*

Batch adsorption isotherm experiments in presence of the contaminants of emerging concern, SMX, ACE and DEET was carried out at room temperature at different pH conditions using 50 mL tubes containing 20 mL contaminant solution (10-50 mg/L) and modified NC (0.1g) as adsorbents. Samples were placed in an orbital shaker set at 250 rpm to maintain uniformity until equilibrium (24 h). Then solutions were centrifuged at 40000 rpm to remove the adsorbent. By determining the concentration of the contaminants before and after the adsorption experiments, the removal efficiency of the adsorbents was calculated using this equation.

$$q_e = \frac{(C_o - C_e)V}{w} \quad (2)$$

Where $q_e$ is the equilibrium adsorption amount (mg/g), $C_o$ is the initial concentration of contaminant solution (mg/L), $C_e$ is the equilibrium concentration of contaminant (mg/L) after adsorption, $V$ is the volume of contaminant solution (L), and $w$ is the mass of modified NC. Emerging contaminant concentrations were measured by HPLC at 25 ºC, flow rate set at 1 mL/min, and the injection volume of 30 µL.

*3.2.1.6.Computational methodological details*

The calculations were carry out based on state-of-the-art density functional theory (DFT) in a plane-wave pseudopotential method as implemented in the Vienna Ab initio Simulation Package (VASP)[84] The Perdew-Burke-Ernzerhof (PBE) exchange-correlation functional with energy cutoff of 400 eV for the plane wave expansion and 4x2x1 Monkhorst-Pack grid for *k*-point sampling are used in the calculations. The long-range interactions (van der Waals) were considered by adding a semiempirical correction to the conventional Kohn-Sham DFT energy, i.e., dispersion-corrected DFT-D3 method of Grimme[85]. The projector augmented-wave pseudopotentials [84, 86] were used for all elements except hydrogen atoms. To better mimic the experimental conditions related with the block copolymer content on NC, an orthorhombic supercell ($a$ = 8.201, $b$ = 20.760, and $c$ = 49.383 Å) was built based on experimental lattice-parameters of bulk-NC [87]. All the atoms were allowed to move during the gradient-minimization procedure without any internal-coordinates constraint while the cell-parameters were fixed. The binding energy (BE) was calculated by using the following formula:

$$|BE| = \left|E_{NC/Pol:CEC} - E_{NC/Pol} - E_{CEC}\right| \qquad 3$$

where, $E_{NC/Pol:CEC}$, $E_{NC/Pol}$, and $E_{CEC}$, means the total (DFT + van der Waals)-energy of the equilibrium structures for adsorbent material + emerging organic contaminant (EOC), the adsorbent material (Jeffamine polymer attach to functionalized NC), and EOC, respectively. The level of accuracy of the present computational methodology is indicated by comparison with high-level many-body theory computations of binding energies for hydrogen-bonded dimers available in the literature[88]. Specifically, the absolute

differences of computed binding energies for formamide and N-methylacetamide dimers are within ~1 kcal/mol.

### 3.2.2. Objective 2. Reusable nanocellulose-block copolymer films for the removal of OECs

#### *3.2.2.1.Modification of CNFs with TMPES and P4VP-PEO*

This process requires a prior hydrolysis of TMPES molecules since hydroxyls groups of CNFs are not acidic enough. In this case, TMPES was hydrolyzed in a polypropylene container by dissolving it (2:1 respect to the mass of CNFs) under magnetic stirring in ethanol/water 80:20 and adding a small drop of acetic acid. Hydrolysis was completed after 2h at room temperature. Amidst the hydrolysis of TMPES, the CNFs solution was dispersed in ethanol/water 80:20 with the addition of a small drop of acetic acid in order to match the conditions of the hydrolysis of TMPES. Once the hydrolysis of the alkoxysilane was completed, CNFs solution was added to the TMPES solution under continuous stirring, and the reaction was left to occur for 24h. CNFs solutions containing P4VP-PEO were prepared following a similar procedure to prepare TMPES-modified CNF. In this case, P4VP-PEO solid was dissolved in CNFs solution at a ratio of 1:1, then added to the previously hydrolyzed TMPES under continuous stirring to obtain a final ratio of 2:1:1 TMPES:CNFs:P4VP-PEO. The reaction was completed after 24h of stirring at room temperature.

*3.2.2.2.Preparation of TMPES-modified CNFs films and TMPES and P4VP-PEO-modified CNFs films*

Once the solution was completely synthesized, ultrasound was employed to obtain a homogeneous dispersed mixture after 10 min. Using vacuum filtration, it was possible to separate the solid materials and obtain the films. To successfully attain the films without breakage, a nylon filter (0.47µm) was first placed into the vacuum filtration system, and then the solution was added. To avoid shrinkage after filtration, each film was dried with nitrogen gas while inside the vacuum filtration system. After this, the film was peeled off from the nylon filter, placed in an oven at 110 °C for 2h, and then stored in a petri dishes (sealed with paraffin sealing film) for further use.

*3.2.2.3.Preparation of CNFs films without modifications*

CNFs films without modifications were prepared by dispersing CNFs in water to obtain 1% wt. suspension. A small drop of acetic acid was added to the dispersion in order to attain the same acidic conditions of the CNFs modification. Suspension was stirred for 24h and homogenized with ultrasound sonication for 10 min. Preparation of the actual films was performed following the same procedure used in *3.3.2.2*.

*3.2.2.4.Characterization of modified CNFs films*

Modified CNFs and CNFs modified films were characterized by Fourier-transform infrared (FTIR) as in section *3.3.1.3.* X-Ray photoelectron spectroscopy (XPS) was used to determine the presence of silicon in the CNFs films due to the modification with TMPES. SEM was used to assay the surface morphology of the films; this analysis was executed in the secondary electron imaging (SEI) mode with 15 kV accelerating voltage.

Wettability of the films was tested by Contact angle measurements performed at room temperature. This process requires that a 1 $cm^2$ piece of CNFs, TMPES-modified CNFs, or TMPES and P4VP-PEO-modified CNFs films was fixed to the stage of the instrument using carbon tape. To start the analysis, a 4.5.0 µL DI water droplet was released from a syringe with a 25-gauge flat needle (0.51 mm inner diameter, 0.26 mm outer diameter) to the surface of the sample. Images of the drop were recorded every 0.5 s up to 120 s (to avoid changes due to evaporation of the drop) and analyses in real-time using Advance software (Version 1.8).

*3.2.2.5.Adsorption batch experiments of SMX using TMPES-modified CNFs films and TMPES and P4VP-PEO-modified CNFs films*

*3.2.2.5.1. Adsorption as a function of time.*

Adsorption capacity of the films with or without P4VP-PEO were measured after placing them in contact with a SMX solution for 1 min, 10 min, 30 min, 60 min, and 240 min. 10 mL of 25 ppm SMX solution was used for each sample and shaken at 250 rpm for the stipulated equilibration time. The absorbance of each sample solution was collected before and after the adsorption using a Thermo Scientific Genesys 10S UV-Vis spectrometer. Using the absorbance values, it was possible to calculate the SMX concentrations and then the equilibrium adsorption amount of the films using equation 2. All experiments were executed in triplicate.

*3.2.2.5.2. Adsorption isotherm experiments.*

Batch adsorption isotherm tests were carried out in triplicate using TMPES-modified CNFs films with and without P4VP-PEO. The prepared solutions ranged from 1 ppm to

100 ppm, and the contact time was set to 1h at neutral pH and room temperature. 10.0 mL of each SMX solution was transferred to 50 mL falcon tubes and a piece of the film was added to the solution. Afterwards, the samples were placed in a shaker at 250 rpm and 25 °C. The absorbance of each sample solution was collected before and after the adsorption and measured using UV-Vis. The equilibrium adsorption amount $q_e$ of the films was calculated using the equation 2. Resulting $q_e$ was plotted as a function of the SMX equilibrium concentration ($C_e$) to perform a fitting with the Freundlich mathematical model.

*3.2.2.5.3. Reusability evaluation of the films*

In order to assay the reusability of the TMPES and P4VP-PEO-modified CNFs films, Samples were immersed in 95 % wt. ethanol to elude the adsorbed SMX. This process was performed at least 5 times in triplicate for samples used in 1h batch adsorption experiments of 10 mL 25 ppm solution of SMX. The same elution procedure was also applied to control samples. The elution time in ethanol was set at 1h in continuous shaking of 250 rpm and 25 ºC. Afterwards, films were rinsed with 200 mL of water to remove the remnant ethanol, dried with compressed air until constant weight and used for another batch adsorption cycle. Equilibrium adsorption amount was calculated and plotted as a function of the cycles.

### 3.2.3. Objective 3. Preparation of porous cellulose tri-acetate membranes with an adsorption active polymer for remediation of EOCs

*3.2.3.1.Preparation of CTA-P4VP-PEO membranes*

CTA membranes reinforced with polyester mesh were prepared by non-solvent induced phase separation (NIPS) process as published elsewhere [89, 90]. Casting solutions were prepared dissolving 17 % wt. CTA and varying concentrations of P4VP-PEO (0, 1 % wt) in 2:1 w/w acetone: DMAc. Solutions were left to magnetically stir at 400 rpm for 48 hours at room temperature. A polyester mesh was attached to a clean glass plate using metal clips and compress air was used to remove dust particles from the mesh surface. Dissolved polymer solutions were casted over the polyester mesh using a film applicator adjusted to 150 μm. Films were allowed to evaporate solvent for approximately 5 s before they were immersed in nanopure water (non-solvent) for 10 min. Finally, membranes were cut to a specific size, rinsed and stored in nanopure water.

*3.2.3.2.Characterization of the membranes*

CTA Membranes were characterized by (FTIR) spectroscopy as stated in section *3.3.1.3.* SEM and contact angle analysis were performed as in section *3.3.2.4.* A computational analysis was used to model the molecules SMX, SDZ, and OMZ in order to generate their electron-density maps. Calculations were performed based on Density Functional Theory (DFT) and geometries of the molecules were optimized at BLYP/6-31G*.

*3.2.3.3.Adsorption batch tests of Sulfamethoxazole, Sulfadiazine, and Omeprazole using the CTA membranes*

*3.2.3.3.1. Adsorption as a function of time*

Adsorption capacity as a function of time of CTA membranes exposed to solutions of 30 ppm of SMX, SDZ, OMZ was performed in a similar way of section *3.3.2.5.1.* OMZ solutions were covered from the light during batch experiments to avoid photo degradation.

*3.2.3.3.2. Adsorption isotherm experiments*

Batch adsorption isotherm tests were carried out in triplicate using CTA membranes exposed to EOCs solutions ranged from 1 ppm to 30 ppm (up to 100 ppm for SMX). The contact time was set to 4 h at neutral pH and room temperature for 30 mL of each solution. OMZ solutions were covered from the light during batch experiments to avoid photo degradation. Other execution parameters and data analysis can be found in section *3.3.2.5.2.*

*3.2.3.3.3. Reusability of the membranes*

Reusability testing of the modified CTA membranes was executed as in section *3.3.2.5.3* for EOCs, SMX, OMZ, and SDZ. OMZ solutions were covered from the light during batch experiments to avoid photo degradation.

CHAPTER FOUR

# 4. EVALUATION OF THE USE OF CELLULOSE-BCP COMPOSITES FOR SORPTION OF EOCs

## 4.1. Introduction

The use of material from natural sources for the adsorption of EOCs has gained considerable attention. Among the wide diversity of bio-materials or bio-polymers, nanocellulose has gained special attention. Nanocellulose (NC) is primarily obtained from naturally occurring cellulose sources, it is inexpensive, biodegradable, practically renewable, and non-toxic [71, 73, 91]. The high amount of primary hydroxyl groups on its surface makes NC a competitive material for the adsorption of contaminants via electrostatic interactions [92, 93]. However, the hydrophobic nature of most of EOCs makes the electrostatic interactions of NC ineffective to remove this type of contaminants. Therefore, it is appropriate to incorporate new functionalities by chemical modification of the NC primary hydroxyl groups in order to improve the adsorption capabilities toward EOCs. Typically, polymers are preferred for this type of modification due to the versatility and variability of their structure that allow them to better interact with a vast diversity of compounds [77]. In terms of the removal of CECs from water, an environmentally friendly and biodegradable polymer such as polyethylene glycol (PEG) represents a feasible option [94, 95]. PEG is a non-toxic polymer widely used as an excipient in pharmaceutical products with high hydrophilicity that allows an easier metabolization of prescribed drugs within the human body [96, 97]. The latter characteristic makes PEG-based polymers an ideal alternative for the removal of CECs, since low water-soluble pharmaceuticals represent a considerable percentage of CECs.

This chapter explores the fabrication of NC grafted with a polyethylene glycol (PEG)-based block copolymer (Jeffamine ED 600). These composites were assessed as feasible materials to adsorb acetaminophen (ACE), sulfamethoxazole (SMX) and N,N-diethyl-meta-toluamide (DEET) as EOCs models from aqueous solutions. NC-Jeffamine composites were prepared by carboxylation of the NC surface via TEMPO oxidation followed by covalent attachment of Jeffamine using EDC/sulfo-NHS reaction. The reaction was followed and confirmed by FTIR and conductometric titration. The physical characterization was performed by thermogravimetric analysis (TGA), Brunauer-Emmett-Teller (BET) analysis, scanning electron microscopy (SEM), dynamic light scattering (DLS), and Z-potential analysis. The adsorption profile of the three EOCs was evaluated by Freundlich and Langmuir models. A computational study based on the density functional theory (DFT) was performed to determine the possible interactions of the EOCs with the material.

## 4.2. Results and discussion

### 4.2.1. TEMPO-mediated oxidation of NC

TEMPO oxidation of NC was performed by varying the molar ratio of NaOCl/AGU to assess the optimal reaction conditions. After the reaction, FTIR was conducted and the intensity of the carbonyl band at 1725 $cm^{-1}$ corresponding to the oxidation process was tracked (see Figure 1a). From the intensity ratios of the carbonyl bands from the FTIR spectra it was possible to determine the optimal concentration of NaOCl to successfully complete the reaction. These results were plotted against the different molar ratios of NaOCl/AGU ranging from 0.05 to 1.0 (Figure 1b). From these results, it was observed that molar ratios higher than 0.5 NaOCl/AGU did not significantly increase the degree of

oxidation. This finding suggests that the limit of possible modifiable hydroxyl groups was reached given the size of the NC particles [80].

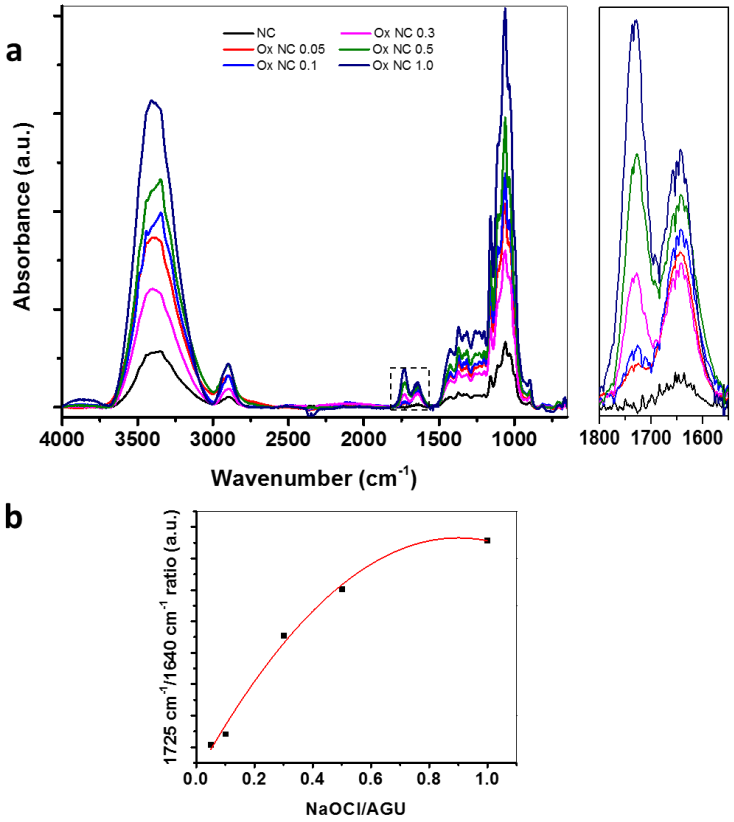


**Figure 1.** a) FTIR spectra of NC and oxidized NC using 0.05-1.0 NaOCl/AGU molar ratios. The highlighted area corresponds to the carbonyl and adsorbed water bands. b) Plot of the 1725 $cm^{-1}$/1640 $cm^{-1}$ height ratios as a function of NaOCl/AGU molar ratios.

The information obtained from the FTIR spectra was compared to the TGA analysis at the different stages of the reaction (Figure 2) and it was shown that the 0.5 NaOCl/AGU molar ratio was enough to significantly decrease the thermostability of NC (highlighted areas). Since NaOCl was the only variable in the different oxidation reactions, it can be argued that NaOCl plays a major contribution in the structural integrity of the NC. Therefore, to maintain the physical integrity of NC, we opted for lowering the molar ratio to 0.3 NaOCl/AGU in order to perform further experiments.

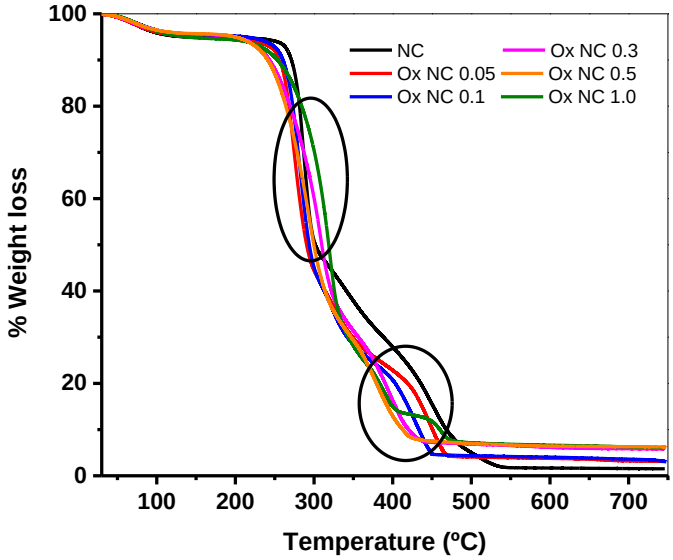


**Figure 2.** Thermograms of NC and oxidized NC using 0.05-1.0 NaOCl/AGU molar ratios.

### 4.2.2. Block copolymer grafting onto oxidized NC

Jeffamine ED 600 is a commercially available block copolymer with a polyether frame consisting of polyethylene glycol and polypropylene glycol with terminal amino functional groups (Figure 3). These types of block copolymers are used to prepare thermo-responsive hydrogels given their hydrophilicity at room temperature and formation of sol-gels at higher temperatures [98, 99]. Here, Jeffamine ED 600 was grafted onto oxidized NC to obtain an enhanced hydrophilic composite with increased adsorption capacities.

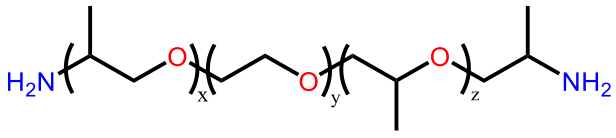


**Figure 3.** Molecular structure of Jeffamine ED 600.

EDC/sulfo-NHS allowed the coupling reaction between the carboxylic groups on the surface of oxidized NC and the primary amines of the Jeffamine to obtain a covalent amide

bond. The ratios of EDC, sulfo-NHS, and Jeffamine (equivalents of $NH_2$) were set to 4 times in relation to the oxidized NC [100]. Figure 4 shows the details regarding the chemical surface changes before and after grafting Jeffamine ED 600 onto the surface of NC.

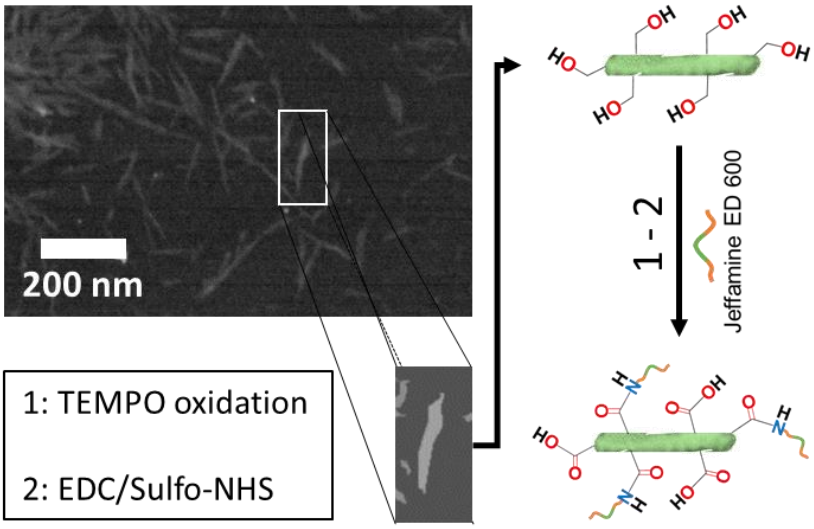


**Figure 4.** Steps for grafting of NC with block copolymer Jeffamine ED 600.

FTIR was utilized to measure the amide functional groups that are expected to form after the coupling reaction. Figure 5 shows the compilation of FTIR spectra of NC (Figure 5a), NC after oxidation (Figure 5b), and NC-Jeffamine (Figure 5c). The pictograms at the right side of each spectrum represent the physical structure of NC highlighting the major functional groups in its surface. After the TEMPO-mediated reaction it can be identified a new intense band around 1600 $cm^{-1}$. This band corresponds to the free salt of carboxyl groups [101], and provides a strong evidence of the oxidation of the NC. Moreover, after polymer grafting, a broad band centered at 1650 $cm^{-1}$ can be observed, which was assigned to the new amide functional group.

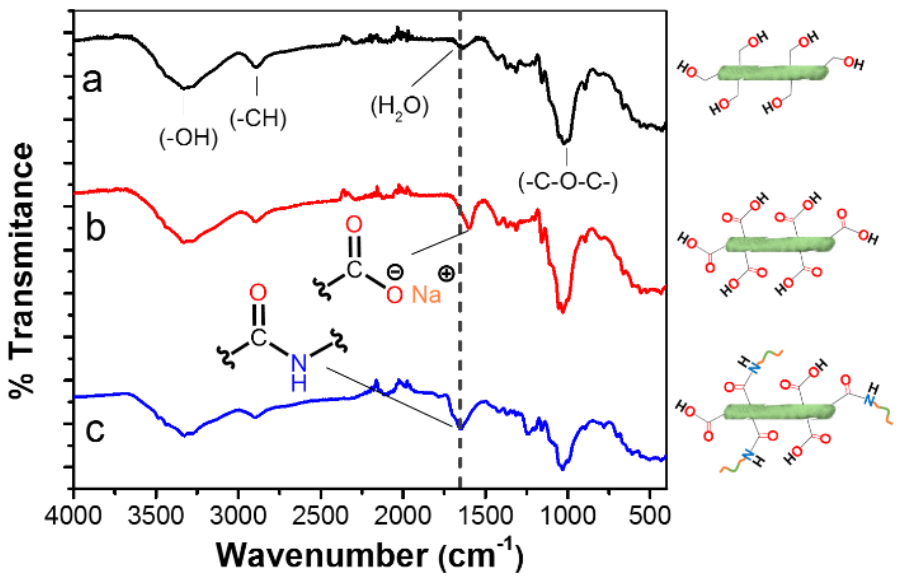


**Figure 5.** FTIR spectra and structural pictograms of (a) NC, (b) oxidized NC, and (c) NC-Jeffamine.

Since the band around 1650 $cm^{-1}$ in Figure 5c appears to be composed of several bands, a Gaussian deconvolution was employed (Figure 6) to better determine the species that were present after the coupling reaction. This deconvolution revealed that this broad band is composed by at least four different bands located at *ca.* 1700 $cm^{-1}$, 1650 $cm^{-1}$, 1600 $cm^{-1}$, and 1550 $cm^{-1}$. The band around 1550 $cm^{-1}$ is characteristic of the bending of N-H, also known as amide II. This band is a confirmation of the formation of the covalent bond between the block copolymer and NC [102]. Additionally, a band at 1600 $cm^{-1}$, corresponding to unreactive carboxylic groups is present in the final sample. This appreciation is reasonable if we take into consideration that this band appears at the same position of that of the FTIR spectrum of oxidized NC. In addition, the statement is reinforced by the fact that molecules might have remained unreacted after the reaction due to steric impediment of the bulky Jeffamine on the surface of NC. Lastly, a band around 1700 $cm^{-1}$ was tentatively interpreted as impurities from the coupling agents sulfo-NHS

and EDC as showed in Figure 7. Here, comparison of the spectra of NC-Jeffamine, EDC and sulfo-NHS suggests that the shoulder at 1700 $cm^{-1}$ matches the intense bands of both coupling agents. This finding could be indicative of a low efficiency of the dialysis process performed to wash the NC-Jeffamine after the reaction was completed. However, it was not expected to play a significant role in the characteristics of the composite.

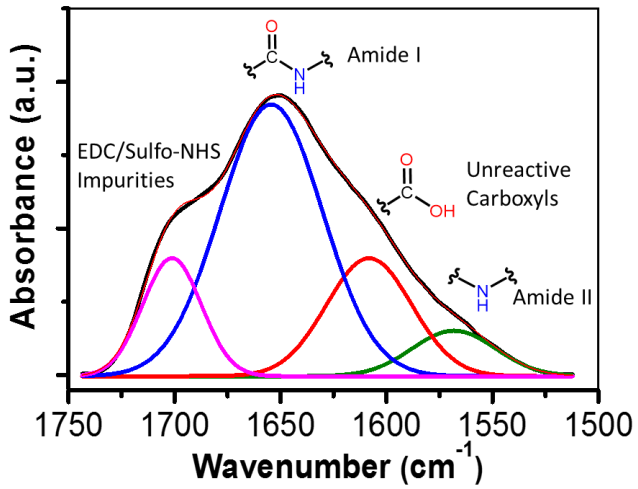


**Figure 6.** Gaussian deconvolution of the broad band around 1650 $cm^{-1}$ of the FTIR spectrum of NC-Jeffamine.

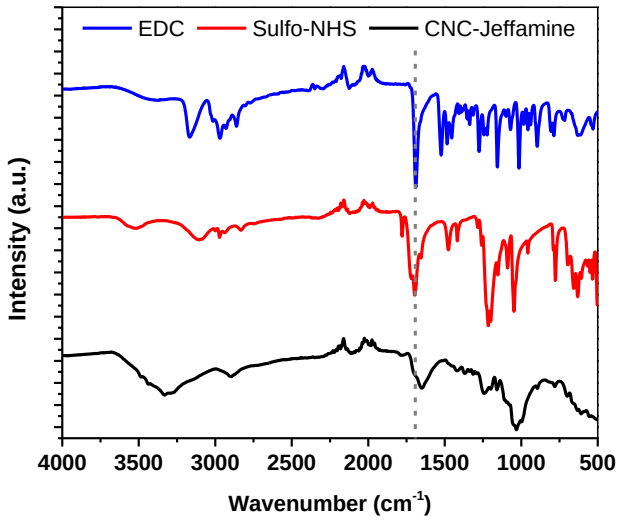


**Figure 7.** FTIR spectra of N-(3-Dimethylaminopropyl)-N′-ethylcarbodiimide (EDC), N-Hydroxysulfosuccinimide sodium salt (sulfo-NHS), and NC-Jeffamine.

After confirmation of the successful grafting, the amount of block copolymer on the surface of NC was determined using conductometric titration. Figure 8 shows the titration plots of oxidized NC and NC-Jeffamine. The initial steep slope in both curves corresponds to the titration of the excess of HCl, followed by a stabilization of the conductivity due to the titration of the available carboxylic acids in the surface of NC. The titration finishes with an increase in conductivity due to the excess of NaOH. After TEMPO oxidation, DO was 0.075, while this value lowered to 0.041 when the block copolymer was grafted. DS of the block copolymer was determined from these results and it was found that the difference between the values before and after block copolymer grafting was 0.033. This value indicates that *ca.* 45% of the carboxylic groups at the NC surface were converted or modified to amide groups. This value is in good agreement with those found in the literature [100].

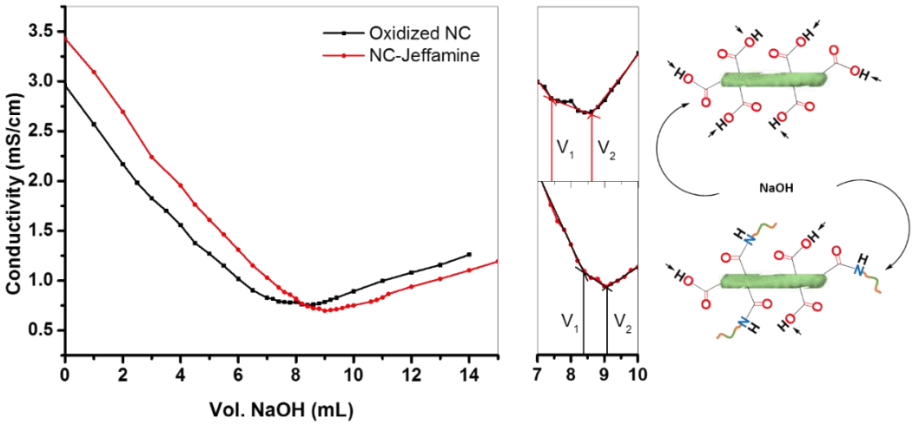


**Figure 8.** Conductometric titration curves of oxidized NC and NC-Jeffamine and pictograms showing their reacting groups.

In order to study the thermal stability of NC and modified NC, TGA was conducted and is shown in Figure 9. Initially, there is a loss of 5 % in mass around 100 ºC, followed by a sharp lost in mass around 300 ºC that slowly decreases until almost no material remains. These changes can also be analyzed using the heat flow plots of Figure 10 that

shows endothermic and exothermic processes as peaks and valleys, respectively. The initial weight loss corresponds to the remained moisture of the sample, while the sharp decrease in mass corresponds to the rapid depolymerization of the outer cellulose chains which is an endothermic process. The last step of the process is characteristic of a hierarchical depolymerization and total carbonization caused by the crystallinity of the NC [73]. It is worth to mention that NC-Jeffamine appears to be less thermally stable than the other species since significant decrease in mass starts around 250 ºC. This can be tentatively caused by the depolymerization of the Jeffamine. However, the heat flow plot of Figure 10 suggests that the last step of depolymerization and carbonization of the NC occurs at higher temperatures. This behavior could be attributed to the possibility that at early state of depolymerization Jeffamine acted as protection of the crystalline structure of NC that now requires more energy to be completely carbonized. Other minor variations in the thermogram trends suggest that the core structure of the NC remains intact suggesting that the oxidation and grafting conditions were adequate for the modification of the NC surface.

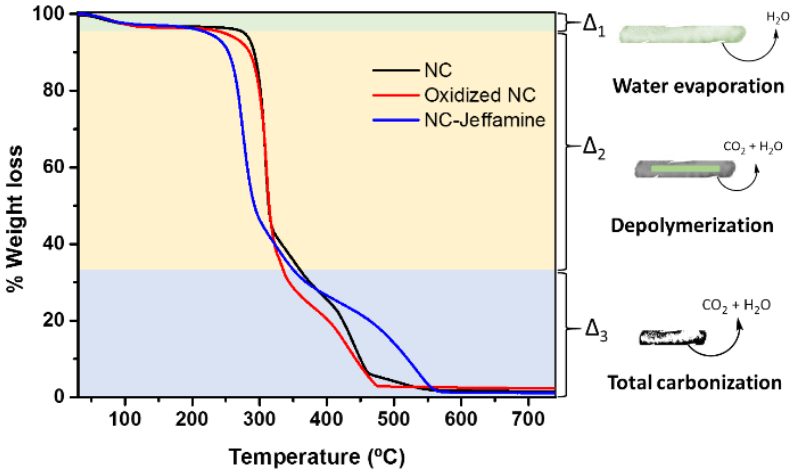


**Figure 9.** Thermograms of NC, oxidized NC, and NC-Jeffamine. The pictograms at the right show the major process during the heating process.

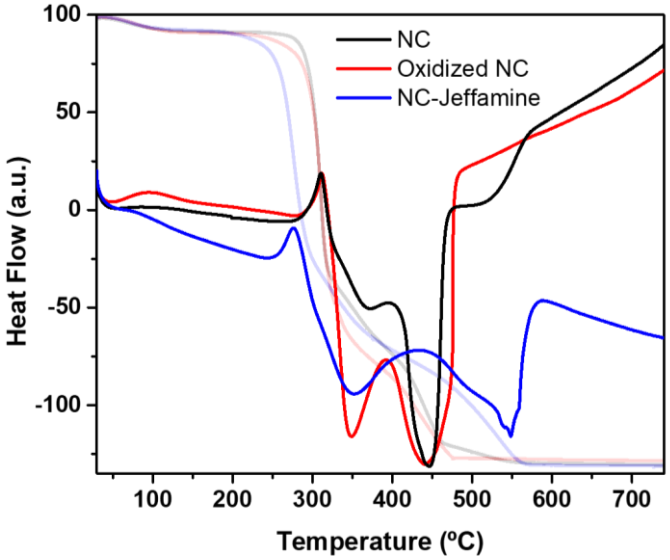


**Figure 10.** Heat flow plots of thermograms of NC, oxidized NC, and NC-Jeffamine.

Chemical characterization was followed by the determination of the surface area of the material before and after the modification. The specific surface areas of NC, oxidized NC, and NC-Jeffamine were measured using the $N_2$ adsorption-desorption method at -196 ºC. The Brunauer-Emmett-Teller (BET) surface area of NC resulted in 2.4 $m^2/g$, 8.4 $m^2/g$ for the oxidized NC, and 15.1 $m^2/g$ for the NC-Jeffamine. These results represent an increase in the surface area after oxidation and grafting of almost 4 and 5 times, respectively, compared to that of NC. Resulting surface area values of NC are consistent with tightly packed and low porous structures due to strong hydrogen bonding [91, 103]. The increase in the surface area after oxidation and grafting can be attributed to the new functionalities (carboxylic groups and block copolymer). It is worth mentioning that NaOCl could have promoted surface roughness due to slight degradation of the glycosidic bonds in NC during the oxidation. However, since NaOCl was not used in the grafting reaction, further increase of the surface area can only be related to the presence of the block copolymer in the NC surface.

SEM images were acquired to account for morphological changes in the sample and would provide more insights on the modification process. From SEM images of NC (Figure 10a), oxidized NC (Figure 10b), and an AFM image of NC-Jeffamine (Figure 10c), it can be observed that the structure of the NC has no significant differences after the oxidation and grafting, respectively. These results suggest that only the surface of NC underwent modification. Moreover, it reinforces the findings from the surface analysis and helps to explain why only a minor increase in the surface area was obtained after the modifications.

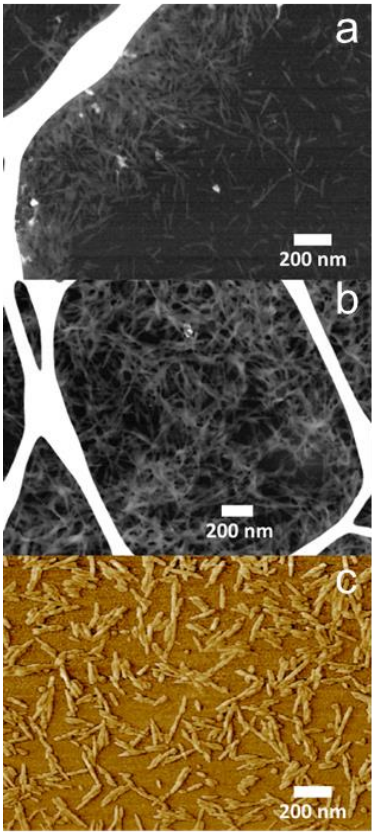


**Figure 11.** SEM images of (a) NC, (b) oxidized NC, and (c) AFM image of NC-Jeffamine.

To characterize NC and modified NC in aqueous solutions, analysis with Dynamic Light Scattering (DLS) and Z-potential was performed to determine the average size and

surface charge, respectively. Figure 11 shows the DLS histograms and Table 1 summarizes the findings for this analysis.

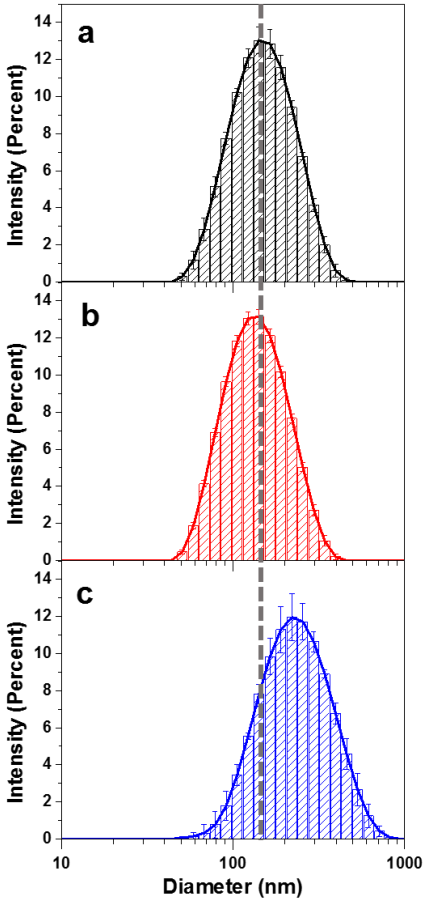


**Figure 12.** DLS histograms of (a) NC, (b) oxidized NC, and (c) NC-Jeffamine.

DLS measures the hydrodynamic diameter of the particles assuming a sphere shape and taking into consideration their translational diffusion coefficient. NC has a rod-like shape, but since the overall translational diffusion coefficient of rods with a defined length are equivalent to the sphere counterparts, the hydrodynamic diameter strongly correlates with the particle length [104]. The measured sizes of NC and oxidized NC are similar, with a slight decrease in the case of oxidized NC. On the other hand, NC-Jeffamine shows a significant increase in the diameter, from 130 nm to 190 nm. These resulting size

distributions showed by DLS analysis are in good agreement with those observed in SEM except for the NC-Jeffamine, which is significantly larger. NC-Jeffamine in aqueous solution has a greater hydrodynamic diameter given the contribution of the extended hydrophilic block copolymer towards the medium. This statement is in good agreement with the other characterization results and at the same time corroborates the successful attachment of the block copolymer Jeffamine ED 600 to the surface of NC.

In the case of the Z-potential results, it is clear that the addition of Jeffamine decreases the surface charge of NC. In this case, the surface charge measured by Z-potential was useful to determine the presence of Jeffamine in the surface of NC. Aqueous dispersion of NC has a surface charge of -54 mV which is related to the presence of negatively charged sulfate groups in its surface that maintain the particles in suspension and avoid aggregation by electrostatic repulsion [73]. After the oxidation, NC surface contains a high concentration of negatively charged carboxyl groups that result in an increase of the negative charge on the surface. On the other hand, the introduction of the neutral Jeffamine polymer substitutes almost 50% of the carboxylates in the surface for amide groups. This explains why the net charge is less negative than the other species.

**Table 1.** Average size and Z-Potential of NC and modified NC.

| Sample | Average size (nm) | Polydispersive index | Z-Potential (mV) |
|---|---|---|---|
| NC | 130 ± 2 | 0.189 ± 0.008 | -54 ± 2 |
| Oxidized NC | 121.0 ± 0.7 | 0.18 ± 0.01 | -58 ± 1 |
| NC-Jeffamine | 190 ± 2 | 0.24 ± 0.05 | -33 ± 1 |

### 4.2.3. Sorption isotherms of EOCs

To measure the adsorption capacity of NC-Jeffamine towards ACE, SMX and DEET, batch experiments were performed at pH 3.0, 7.0 and 9.0. Adsorption isotherms data were fitted to the mathematical non-linear models of Langmuir and Freundlinch [105]. Results are presented in Table 2. For ACE, there was no significant adsorption at acidic pH, whereas at neutral and basic pHs adsorption was evident, being higher at basic conditions. However, for SMX higher adsorption was observed at both acidic and basic pHs, with pH 9.0 being slightly higher. On the other hand, DEET adsorption increased as a function of pH. In terms of the mathematical models, ACE had a better fitting with the Freundlich model at basic pH, meanwhile, SMX had a better fitting at acidic pH with both Langmuir and Freundlich models. DEET was consistent along the pH range measured, being the Freundlich models the one that presented a better fit. Batch adsorption experiments using NC or oxidized NC were not successful, since no significant adsorption was obtained (Table S1).

Table 2. Isotherms plot for the adsorption of EOCs at different pHs.

| Emerging contaminant | pH 3 | pH 7 | pH 9 |
|---|---|---|---|
| Acetaminophen | 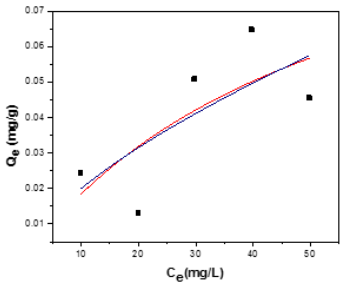 ----- Langmuir $R^2$: **No Fit** ----- Freundlich $R^2$: **No Fit** | 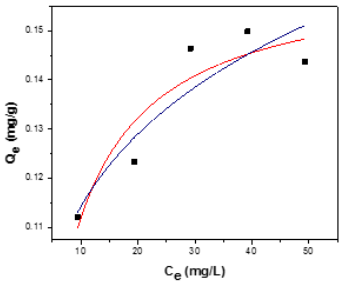 ----- Langmuir $R^2$: **0.82** ----- Freundlich $R^2$: **0.79** | 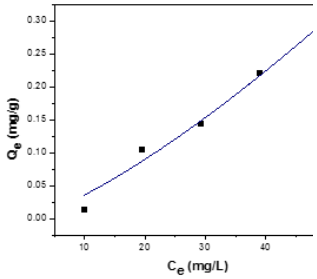 ----- Langmuir $R^2$: **No Fit** ----- Freundlich $R^2$: **0.97** |
| Sulfamethoxazole | 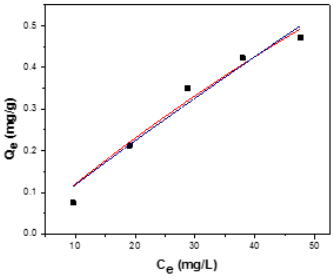 ----- Langmuir $R^2$: **0.96** ----- Freundlich $R^2$: **0.95** | 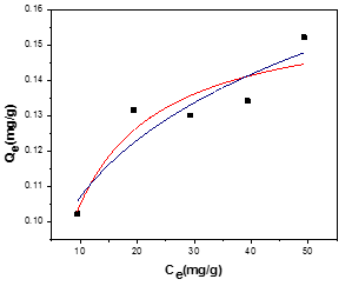 ----- Langmuir $R^2$: **0.82** ----- Freundlich $R^2$: **0.81** | 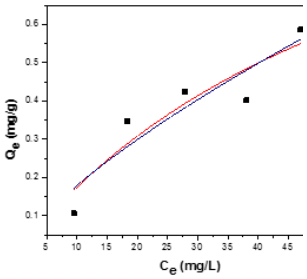 ----- Langmuir $R^2$: **0.82** ----- Freundlich $R^2$: **0.81** |
| DEET | 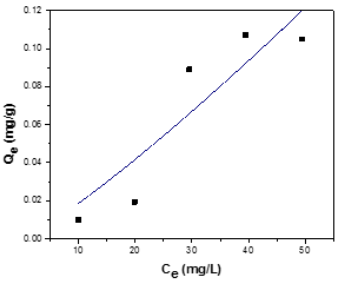 ----- Langmuir $R^2$: **No Fit** ----- Freundlich $R^2$: **0.77** | 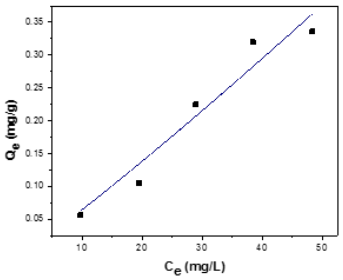 ----- Langmuir $R^2$: **No Fit** ----- Freundlich $R^2$: **0.93** | 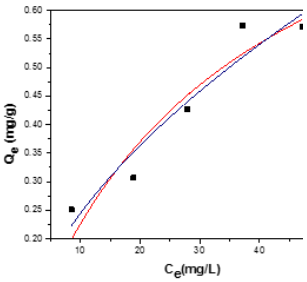 ----- Langmuir $R^2$: **0.87** ----- Freundlich $R^2$: **0.90** |

To analyze the adsorption isotherms of the different EOCs, it is important to take into consideration the structural changes that both NC-Jeffamine and EOCs undergo at different pHs. Due to the presence of unreactive carboxylic groups in the surface of NC-Jeffamine, the dispersion of the particles in aqueous solution is affected by pH. As seen in Figure 12, at acidic pH the particles are in an aggregated state forming a viscous slurry. This phenomenon occurs due to protonation of the carboxylates to form neutral carboxylic acids.

At this condition, hydrogen bonds overcome the electrostatic repulsions of the particles. As the pH increases, the formation of negatively charged carboxylates restores the electrostatic interactions of the particles to obtain well-defined aqueous suspensions. The adsorption of all of the EOCs increases at pH 9 as seen in Table 2. It can be suggested that the better dispersity of NC-Jeffamine in the solution favors the interaction with the contaminants and enhances the adsorption.

In the case of EOCs, the pKa plays an important role in the solubility and the net charge of each one. ACE has a pKa of 9.5 [106], which means that at a basic pH it has a net negative charge. That behavior can explain why there is almost no adsorption at pH 3 since it is possible that ACE remained insoluble in the aqueous solution. This phenomenon decreases the possibility of effective interactions with NC-Jeffamine. SMX and DEET have acid pKa values of 5.6 and 2.0, respectively [107]. Besides the aggregation of NC at acid pH, the adsorption of SMX is considerable. In this case, the adsorption must be driven by electrostatic interactions of positively charged sulfamethoxazole and the surface of NC-Jeffamine. This behavior is useful to understand the relatively good fitting of both Langmuir and Freundlich models, especially considering the formation of consecutive layers of ions of SMX on the surface of aggregated NC-Jeffamine [108] . On the other hand, the adsorption of DEET is more consistent with the increase of the solution pH. In this case, its lower pKa avoided the formation of charge species under the studied conditions. That situation suggests that mostly non-specific interactions are possible between DEET and NC-Jeffamine and at the same time explain the poor correlation with the two mathematical models.

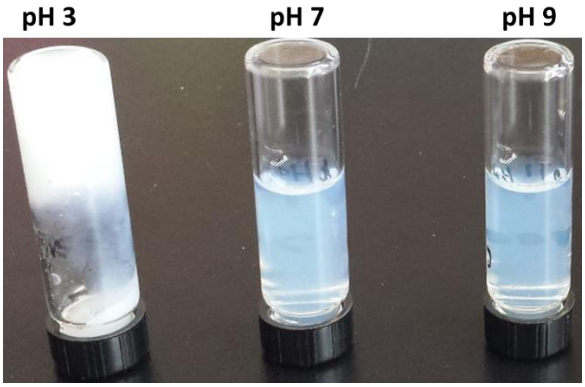


**Figure 13.** NC-Jeffamine aqueous suspensions at different pHs.

### 4.2.4. Computed binding energies

Based on the finding that the experimental adsorption of EOCs onto NC and oxidized NC was negligible in this study, the computational effort was focused on NC-Jeffamine. Figure 13 shows the atomistic models for oxidized NC surface (composed by 4 chemical-formulas of oxidized cellulose), a supercell containing 4-unit-cells of NC-Jeffamine, and the equilibrium structure for adsorption site of ACE onto NC-Jeffamine. The elucidation of the minimum-energy atomistic structures and binding energies computationally obtained helps to understand how the adsorption of EOCs onto NC-Jeffamine is taking place and the nature of interactions between them. A variety of intermolecular interactions, such as moderate hydrogen bonds and van der Waals (vdW) forces are the reason for adsorption of EOCs onto NC-Jeffamine. In the case of ACE two hydrogen bonds (hb1 and hb2) are stablished (see Figure 13), the bond lengths are 2.02 Å for hb1 and 2.29 Å for hb2 and the contribution of vdW-interactions to its binding energy is 14.5 kcal/mol of 21.2 kcal/mol. For SMX, one hydrogen bond is made with a bond length of 2.28 Å (see Figure 14a) and the vdW contribution to binding energy is 7.2 kcal/mol of 14.3 kcal/mol. Finally,

for DEET, the contribution to binding energy is due almost to the vdW-interactions which account for 5.7 kcal/mol of the 8.4 kcal/mol total binding energy (see Figure 14b). In all the cases, the adsorption of EOCs onto NC-Jeffamine do not affect the atomistic structure of overall NC-Jeffamine drastically, this can be observed by direct comparison of Figure 13c and Figure 14.

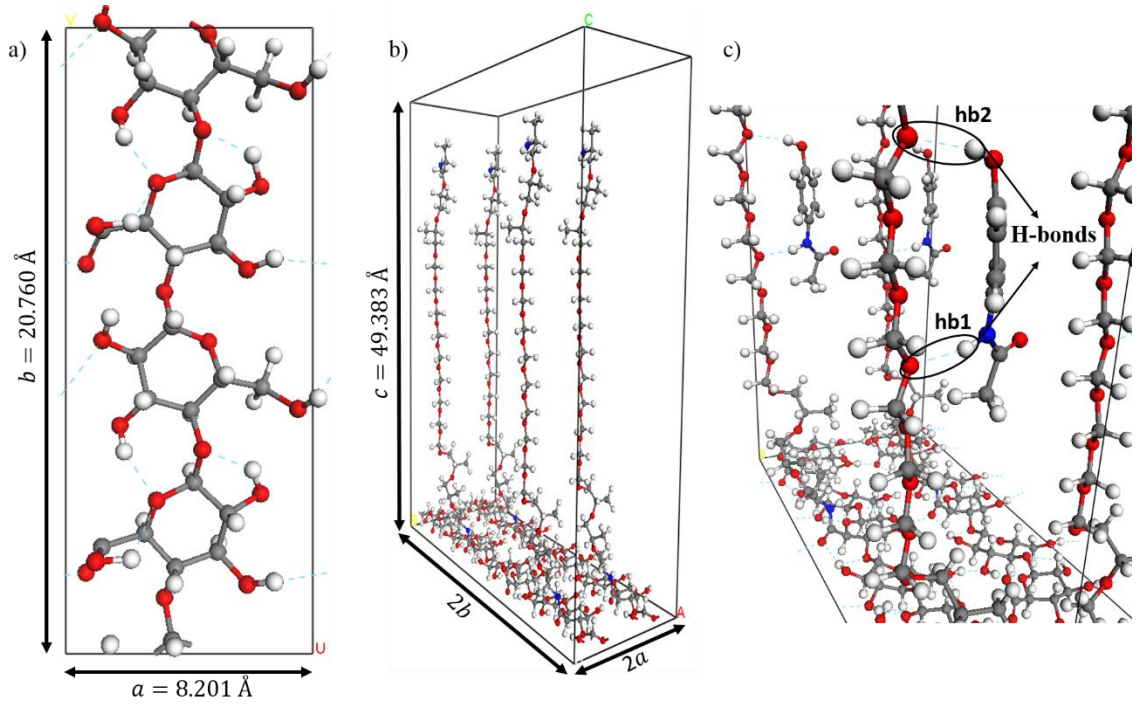


**Figure 14.** Atomic structures models for (a) 1x2-surface of oxidized NC, (b) 2x2x1 supercell of NC-Jeffamine, and (c) a 2x2x1 supercell representation of minimum-energy structure for Acetaminophen adsorbed on NC-Jeffamine through two hydrogen bonds.

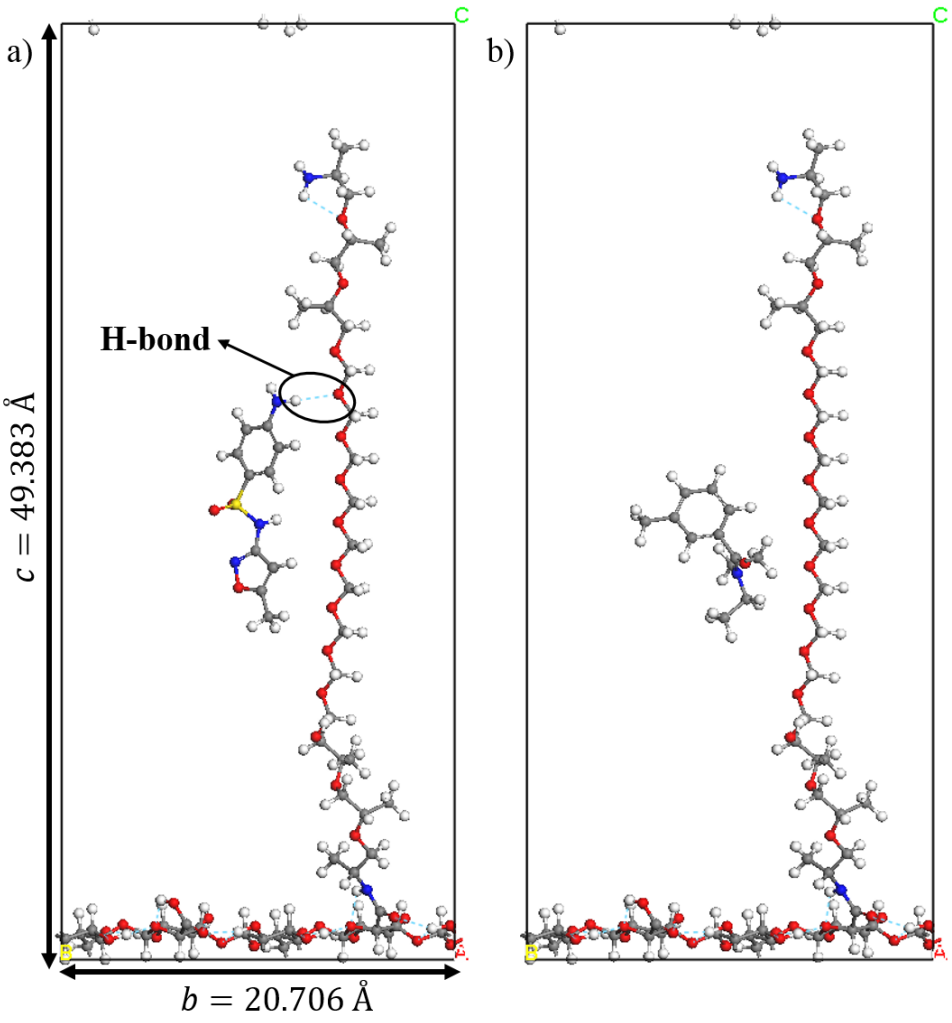


**Figure 15.** Atomic structures models for unit-cell representation of minimum-energy structures for (a) SMX and (b) DEET adsorbed on NC-Jeffamine.

### 4.3. Conclusions

It was demonstrated the feasibility of the adsorption of EOCs using the environmental-friendly NC-Jeffamine by means of experimental methods (adsorption isotherms) and computational methods (atomistic structures and binding energies). Jeffamine was successfully attached to oxidized NC to obtain nanoparticles with similar aspect ratio to that of the precursor, as suggested from SEM imaging and DLS analysis, but with higher surface area (BET analysis). These new physical properties allowed the adsorption of ACE,

SMX, and DEET at pH 3, 7, and 9 by means of electrostatic interactions with the polymer arrangements in the surface of the nanoparticle. The computational calculations resulted in binding energies of 21.2 kcal/mol, 14.3 kcal/mol and 8.4 kcal/mol for ACE, SMX and DEET, respectively, related to hydrogen bonds and/or van der Waals interactions with the polymer chain. These computational results clearly indicate the adsorption of EOCs onto NC-Jeffamine at the molecular level and are in agreement with the adsorption trends that were experimentally obtained at neutral pH. This analysis has placed a fundamental basis on the production of eco-friendly materials based on polymer grafting and their use for the remediation of contaminants from aqueous media.

CHAPTER FIVE

# 5. REUSABLE NANOCELLULOSE-BLOCK COPOLYMER FILMS FOR THE REMOVAL OF EOCs

## 5.1.Introduction

NC are typically used as a supporting composite due to its unique structure that consists of a long chain of glucose, with an outskirt of hydroxyl groups [109]. These hydroxyl groups can be exploited to efficiently modify the surface of NC with chemical functionalities in order to enhance specific interactions with a wide variety of contaminants. One of the water remediation strategies that take advantage of the characteristics of NC is the adsorption. NC has been extensively used for adsorption in water of heavy metals [110-113] and dyes [114-116] by means of electrostatic interactions between the aqueous ions and charged functional groups added to the NC surface. Unfortunately, this approach if not suitable for the adsorption of organic contaminant with low polarity. This drawback has been addressed by the preparation and modification of highly porous NC aerogels [117] that based the removal of hydrophobic contaminant by entrapment in their structure [118]. However, preparation of those materials requires the use of expensive and time-consuming supercritical, freeze-drying or solvent exchange. Moreover, the remediation mechanism involves diffusion into the structure which could make difficult the regeneration and reuse of the material.

A possible way to enhance the adsorption of NC against organic contaminants involves the functionalization with materials that address the adsorption by specific interactions. This improvement can be accomplished by the addition of suitable block copolymers (BCPs), materials that have gain special attention in recent years in terms of remediation

[119-121]. Block copolymers are potential candidates for modification of NC intended for water remediation due to their enhanced functional properties. This is possible because these polymers can be configured into a nearly infinite number of molecular architectures based on the composition and molecular weight of its constituting monomers [29, 122]. This versatility can allow the BCPs to interact with organic contaminants through physical and chemical interactions such as electron donor-acceptor that can be reversed allowing the reuse of the material [123].

Handling of a material after adsorption is an important factor that determine its feasibility for large scale operation. It is well known that NC is easily dispersed in aqueous solutions due to its hydrophilicity [78]. This characteristic translates into the use of high-speed centrifugation to remove it from the solution and sonication to avoid agglomeration for further reuse. Nevertheless, addition of hydrophobic moieties to the NC surface has proved to be effective to overcome this shortcoming. There are several reports that employ alkoxysilanes[124] to stabilize NC in water, and at the same time imparting super hydrophobic characteristics for the removal of oil from water [125-127].

In this chapter a novel material prepared by the modification of CNFs with the alkoxysilane trimethoxy(2-phenylethyl)silane (TMPES) and the addition of poly(4-vinylpyridine-b-ethylene oxide) (P4VP-PEO) is presented. This material was used to fabricate films by a simple vacuum-filtration method and then employed for the adsorption of sulfamethoxazole (SMX) as a model EOC in water. CNFs are composed by fibers with diameter in the range of 5-50 nm and length of several micrometers that can form intricate structures due to the crosslinking that ultimately define the films [128].These films are completely stable in water since the phenyl groups provided by the silane confers

hydrophobicity to the CNFs surface. Additionally, the P4VP-PEO present in the structure can interact with SMX by means of electron-donor-acceptor (EDA) interactions to complete the adsorption process. Finally, these films can be reusable by applying a simple method of immersion of the material in ethanol to elude the SMX, rinsing it with water, and drying at room temperature.

## 5.2.Results and Discussion

### 5.2.1. Modification of CNFs with TMPES and P4VP-PEO

Although alkoxysilanes with a wide range of functionalities have been continuously used as coupling agents to promote the adhesion of different polymeric surfaces [124], in this investigation an alkoxysilane was aimed to enhance the stability of CNFs in aqueous solution. Previously, composites of nanocellulose grafted with a block copolymer were prepared intended for the adsorption of EOCs. This composite was easily dispersed in aqueous solution, making their removal after the adsorption difficult and time-consuming [129]. Modifying the surface of CNFs with a hydrophobic functionality limits the solvation of the cellulose, making it stable against dispersion. A silane compound, TMPES, was selected (Figure 15a) mainly due to its hydrophobic phenyl arm that is separated from the silane by two carbons. This characteristic is likely to help in lowering the steric repulsion during the reaction.

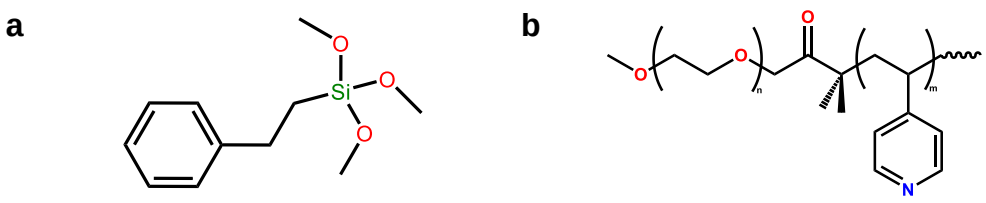


**Figure 16**. Molecular structure of a) TMPES and b) P4VP-PEO.

Due to the lower acidity of cellulosic hydroxyl groups present in CNFs, TMPES would have been unable to form covalent bonds in the CNFs surface [130]. For that reason, it was necessary to first hydrolyze the trimethoxy groups in TMPES to form silanols. This step also promotes the formation of -Si-O-Si- bonds that are resistant to hydrolysis; consequently, they are unable to react with CNFs. Brochier-Salon *et al,* studied the kinetics of hydrolysis of several alkoxysilanes (TMPES included) under acidic conditions using $^{29}$Si NMR. This study found that after approximately 3 h *ca.* 92% of silanol sites are still available with some formation of -Si-O-Si- groups [131]. Based on those findings, we carried out the hydrolysis for 2 h to avoid the presence of -Si-O-Si-. Thus, the resulting silanols would be available to interact with the hydroxyl groups of the CNFs surface via hydrogen bonds. These interactions are reversible, but heat treatment at 110 ºC for 2 h is sufficient to form irreversible -Si-O-C- bonds [124].

Once modified, the TMPES-CNFs composite can provide a support for the active adsorbent, P4VP-PEO (Figure 15b). P4VP-PEO is a block copolymer that is responsive to pH due to protonation/deprotonation of the pyridyl group. Also, slight changes in temperature can promote intermolecular interactions of the ethylene oxide chains [132]. Here, we take advantage of the high electron density of the pyridyl groups of the block copolymer to adsorb low electron density EOCs such as SMX. By means of electron-donor-acceptor (EDA) interactions [133], it is possible to remove the SMX from aqueous solution. Since these types of interactions are reversible, it would enable the reversed adsorption reaction with a simple solvent exchange, and thus allow the reuse of the material (Figure 16c). The addition of solid P4VP-PEO was performed during the reaction of silanols with CNFs. This mixture led to the formation of a matrix where the hydrophilic

ethylene oxide chains interact with CNFs and the vynilpiridyl functionalities interact with the phenyl groups of the silane (Figure 16a). Figure 16b shows the actual CNFs films after the modification. It can also be noted that after immersion in water, films can adsorb the liquid despite of the hydrophobic modification. Interestingly, when CNFs films without modification were shaken in water at 250 rpm for 24 h, the films dispersed in the solution, while TMPES-modified CNFs films remained undamaged (Figure 17).

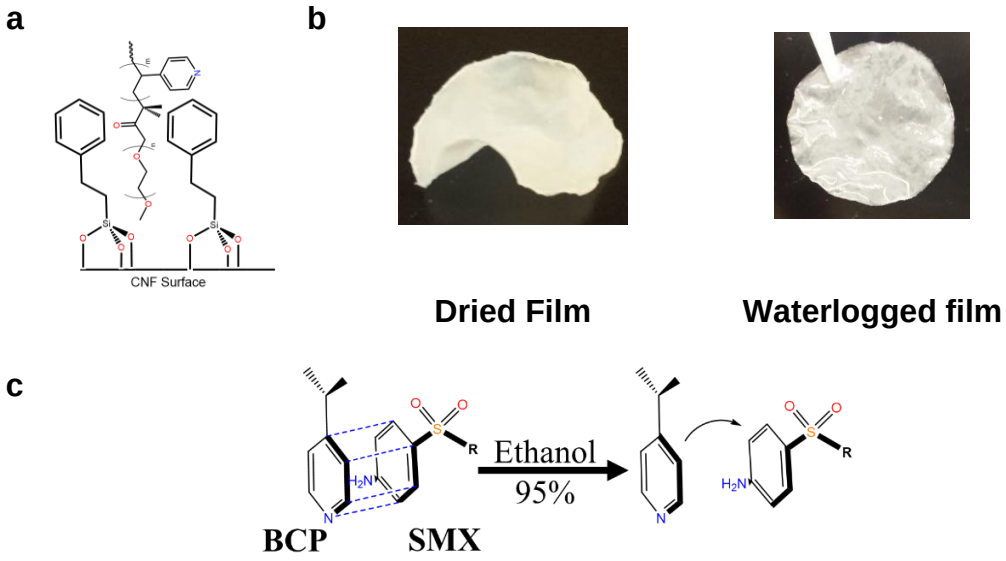


**Figure 17**. a) Molecular structure of TMPES covalently attached to the surface of CNFs showing the presence of P4VP-PEO. b) photographs illustrating the dried and waterlogged CNFs films. c) schematic of the EDA interaction of pyridyl ring of P4VP-PEO with the substituted phenyl group of SMX and its elution with ethanol.

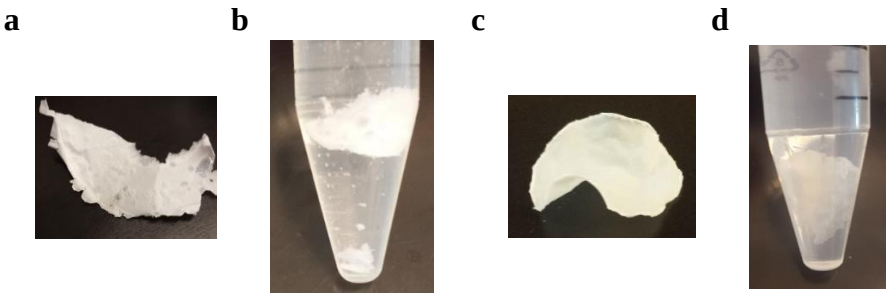


**Figure 18.** a) and c), CNFs film with and without TMPES, respectively. b) and d), films after shaking in water for 24 h at 250 rpm and 25 ºC.

### 5.2.2. Characterization of the modified CNFs films

CNFs and TMPES-modified CNFs were characterized using XPS (Figure 18) in order to identify the silicon signal related to the Si-O-C bonds formed during the modification of CNF with the alkoxysilane. The XPS spectrum of the TMPES-modified CNFs clearly shows the peaks corresponding to Si 2s at around 150 eV and Si 2p at 100 eV. These peaks are not present in the XPS spectra of CNFs, confirming the successful addition of TMPES.

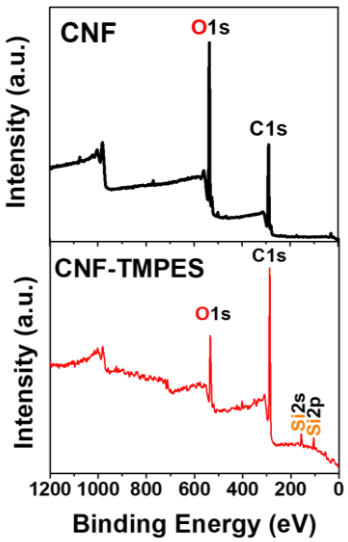


**Figure 19**. XPS spectra of CNFs and TMPES modified CNFs films.

Deconvolution of C1s XPS spectrum of CNFs films shows four peaks that are characteristic of cellulose materials [134] (Figure 19a). The peak at 284.8 eV corresponds to C-C and C-H bonds. The peak at 286.7 eV is related to carbon atom bond to a single oxygen atom. This peak in general is the most intense due to the large amount of hydroxyl groups in the cellulose structure. The peak at 288.4 eV corresponds to carbon atom bond to two oxygen atoms. The peak at 290.4 eV represents a carbon atom linked to one carbonyl oxygen and one non-carbonyl oxygen. The fitted C1s XPS spectrum of TMPES-modified CNFs films shows the same peaks as CNFs in addition to one new peak at 287.8 eV (Figure 19b). This peak is possibly related to the new bond between Si-O-C obtained after the modification with the alkoxysilane. This type of bond is also found in the deconvolution of Si 2p spectrum of TMPES-modified CNFs films (Figure 19c). Here, the peak at 103.2 eV represents one silicon atom bond to one oxygen atom that at the same time is linked to one carbon (Si-O-C) [135]. In addition, the peak at 101.7 eV suggests that there is polymerization of the silane in the surface of CNFs, due to the formation of Si-O-Si bonds [136]. However, this polymerization is small compared to the formation of the covalent bonds with CNFs if we consider the intensity of the Si-O-Si and Si-O-C peaks.

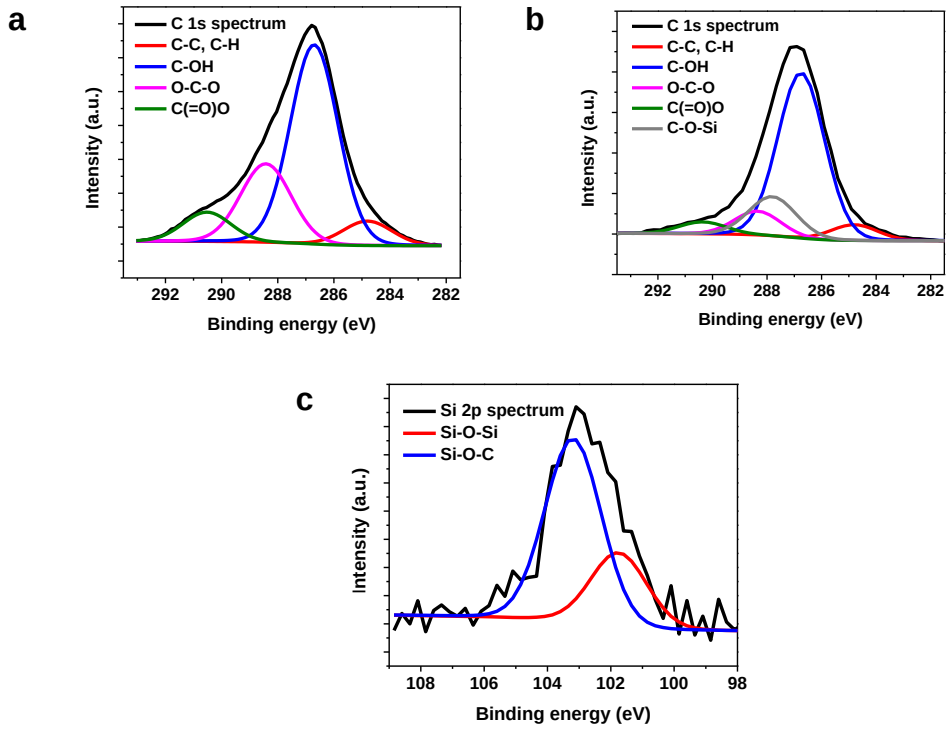


**Figure 20**. Fitted high resolution C 1s XPS spectra of CNFs (a) and TMPES-modified CNFs films (b). Fitted high resolution Si 2p XPS spectra of TMPES-modified CNFs films (c).

FTIR was used to identify the critical functional group vibrations of the different components of the modified CNFs films compare to those of the precursors (CNFs, TMPES, and P4VP-PEO). Figure 20 shows the spectra of CNFs highlighting their characteristic functional groups. A signal observed at 3300 $cm^{-1}$ is assigned to the hydroxyl stretching vibration (OH-), the band at 2800 $cm^{-1}$ corresponds to the stretching vibrations of the methylene groups ($CH_2$-), while a sharp band around 1100 $cm^{-1}$ corresponds to the glycosidic ring stretching. The presence of a small band around 1650 $cm^{-1}$ which is related to adsorbed water is also common. Despite of the modification of CNFs with TMPES, the FTIR spectrum of these films did not show any band related to the phenyl groups of the silane around 1450 $cm^{-1}$. These bands are overlapped by the region of the CNFs hydrogen bending that ranges from 1300 $cm^{-1}$ to 1500 $cm^{-1}$. The same effect occurred to the silicon

signal expected from 500 $cm^{-1}$ to 1000 $cm^{-1}$ [137]. In the FTIR spectrum of the CNFs films modified with TMPES and P4VP-PEO, it was possible to identify two bands at 1415 $cm^{-1}$ and 1596 $cm^{-1}$ [138]. These bands correspond to the vibrations of the pyridine ring that are also present in the spectrum of P4VP-PEO. This is clear evidence that suggests the successful addition of P4VP-PEO to the CNFs films.

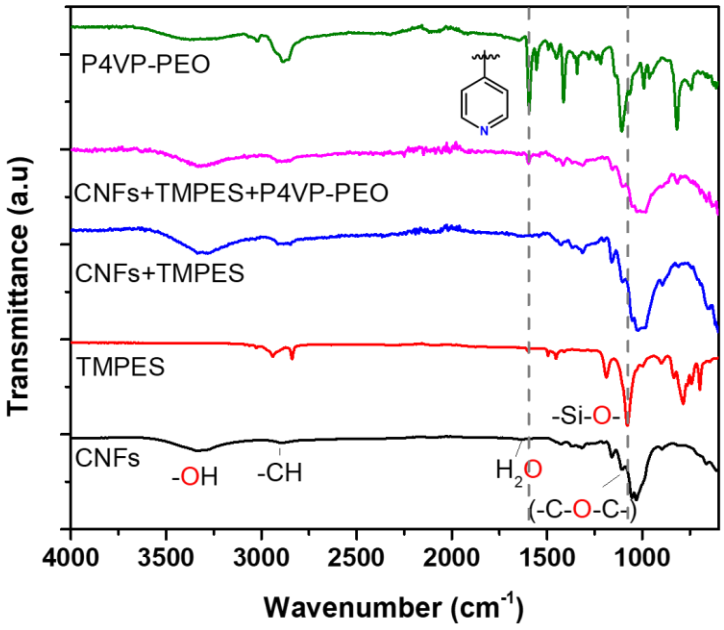


**Figure 21**. FTIR spectra of CNFs, TMPES, P4VP-PEO, CNFs + PEMS and CNFs + PEMS + P4VP-PEO.

Contact angle (CA) measurements were used to estimate the wettability of CNFs films and CNFs with the respective modifications (Figure 21). The phenyl group in TMPES acts as a hydrophobic group that makes the solvation of cellulose fibers difficult. This behavior can be observed in Figure 21b, which shows a CA of 85º for TMPES-modified CNFs films at time 0. After 120s, the value decreased to 66º due to water penetration via diffusion through the film. This result is directly related to the ratio of TMPES/CNFs used for the modification that is critical to gradually wet the films and avoid their dispersion in aqueous

solution. In contrast, the water droplet penetrated the CNFs film without modification almost immediately after it came in contact with the surface (Figure 21a). After 120s, the film started to separate from the surface. This phenomenon is a consequence of the swelling of the material due to high hydrophilicity of cellulose that leads to the penetration of water molecules [139]. TMPES and P4VP-PEO-modified CNFs films (Figure 21c) had higher wettability compared to CNFs films modified with TMPES. Here, the CA was 56º, which remained steady during the measurement. This increase in the wettability is likely an effect of the polyethylene oxide chains in P4VP-PEO that add hydrophilicity to the films [140].

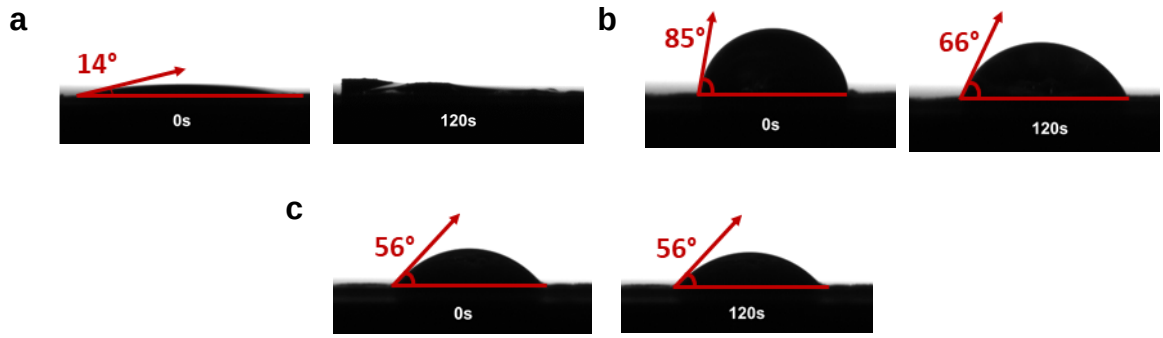


**Figure 22.** Contact angle measurements of a) CNFs films, b) TMPES-modified CNFs films, and c) TMPES and P4VP-PEO-modified CNFs films.

SEM micrographs of TMPES and P4VP-PEO-modified CNFs films show a rough morphology along the surface (Figure 22). A closer inspection of the images reveals that the surface is composed of tightly agglomerated fibers that are randomly distributed. This is an effect of the method used to prepare the films. Initially, components are suspended in the solution, but once the vacuum filtration begins, modified cellulose fibers accumulate layer-by-layer as shown in the cross-section image of the films (Figure 22e). These micrographs also reveal that the films are quite monolithic with minimal observable

porosity, suggesting that only P4VP-PEO found in the surface of the films is readily available to interact with SMX.

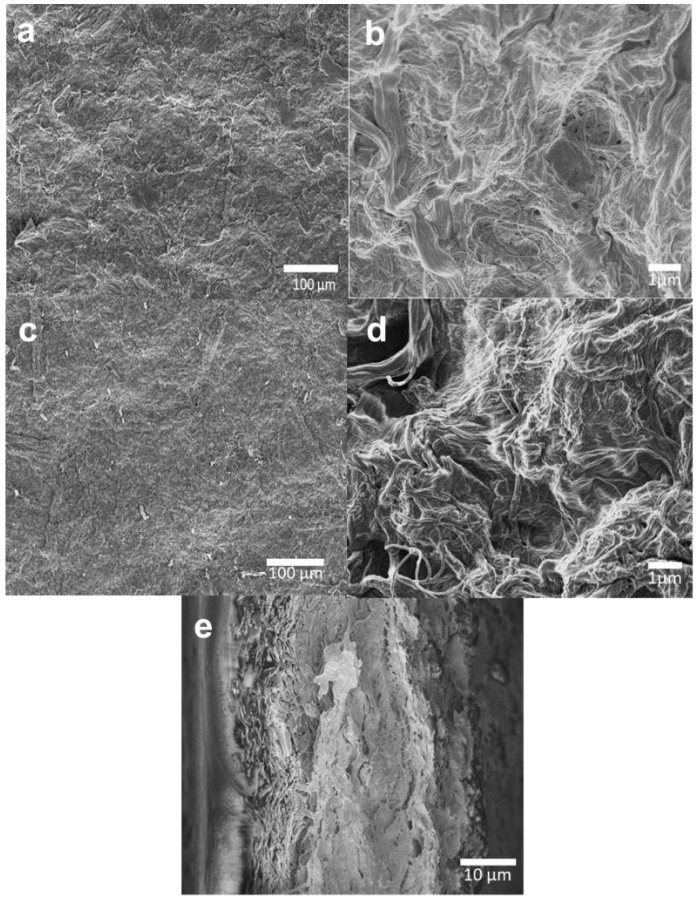


**Figure 23**. SEM micrographs of a) frontside, c) backside, and e) cross-section of TMPES and P4VP-PEO-modified CNFs films. Higher magnification of the frontside and the backside are showed in b) and d), respectively.

### 5.2.3. Adsorption batch experiments of SMX using TMPES-modified CNFs films and TMPES and P4VP-PEO-modified CNF films

Batch experiments were performed in order to assess the adsorption capacity of TMPES and P4VP-PEO-modified CNFs films against SMX as EOC model compound. Batch experiments using TMPES-modified CNFs resulted in a negligible adsorption, which suggests that only P4VP-PEO is able to adsorb SMX (Figure S1).

*5.2.3.1.Adsorption as a function of time*

The effect of equilibration time on the adsorption of SMX using TMPES and P4VP-PEO-modified CNFs films is shown in Figure 23. This graph displays low $q_e$ when equilibrium adsorption time was set to 1 min. However, taking the measurement error into consideration, the difference between this point and higher equilibration times is minimal; therefore, most of the adsorption could be occurring on the surface of the films. This outcome is supported by the CA measurements data and SEM images that showed a low water penetration and a tightly packed structure, respectively. Figure 23 (right) shows a representation of SMX adsorbed on the surface of the modified CNFs films where P4VP-PEO is readily available. If we follow the trend line of the plot in Figure 23, the optimal adsorption equilibrium time is reached at approximately 60 min. After this point, higher equilibrium times did not cause a significant change in $q_e$. Consequently, 60 min was used as a default adsorption equilibrium time for further batch adsorption experiments.

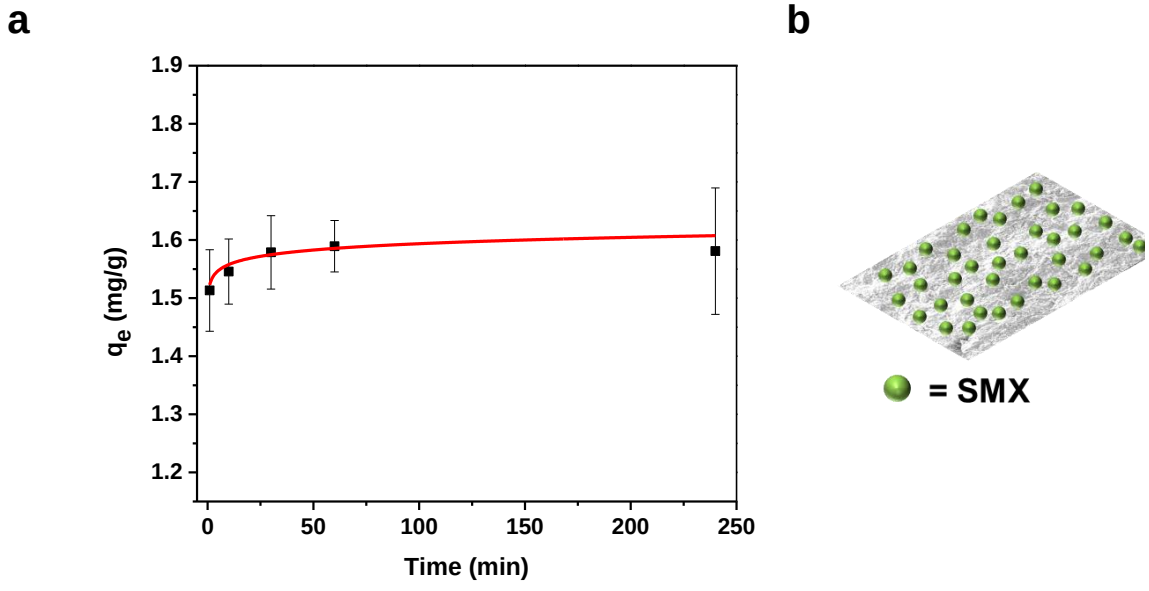


**Figure 24.** Adsorption capacity of TMPES and P4VP-PEO-modified CNFs films as a function of time (a), with a representation of the superficial adsorption of SMX (b).

*5.2.3.2.Sorption isotherms of SMX*

The adsorption isotherm of SMX using TMPES and P4VP-PEO-modified CNFs films was obtained at equilibrium time of 1 h, neutral pH, and room temperature. After determining the $q_e$ and the SMX equilibrium concentration ($C_e$), the resulting plot was fitted with the Freundlich mathematical model. The Langmuir model was also utilized, but a poor fitting suggested a distribution of active adsorbent sites rather than formation of a homogeneous monolayer at adsorption equilibrium [141]. The Freundlich isotherm model is an empirical equation introduced to describe the processes of adsorption. In this expression,

$$q_e = K_f C_e^{1/n} \quad (4)$$

$q_e$ represent the equilibrium adsorption amount (mg/g), $K_f$ and $n$ are empirical constants that are related to the adsorption magnitude and effectiveness, and $C_e$ is the concentration in equilibrium (mg/L). Figure 24 (left) shows the non-linear fitting of the $q_e$ as a function of the $C_e$. This fitting suggested that the modified film had not reached its maximum adsorption capacity. Unfortunately, it was not possible to determine the maximum adsorption capacity for two reasons: at higher concentrations of SMX is unstable in aqueous solution (see Figure S2) and a reduction of the mass of the films used in the adsorption experiment may result in higher deviations. The linear form of the Freundlich equation

$$lnq_e = lnK_f - \frac{1}{n} lnC_e \quad (5)$$

can be used to determine $K_f$ and $n$ (Figure 24, right). In this case, $n$ was determined to be approximately 4.3. In general, values of n > 1 are common and suggest that the adsorption proceeded by physical interactions, and that agrees with our hypothesis of the EDA interactions between SMX and modified CNFs. Moreover, $n$ values between 1-10 can generally be related to satisfactory adsorptions [142].

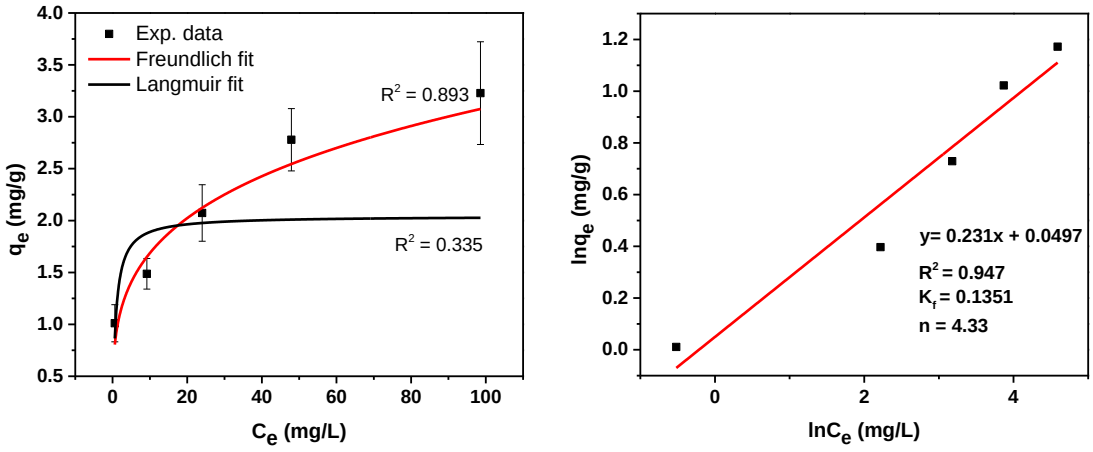


**Figure 25.** Adsorption isotherm of SMX using TMPES and P4VP-PEO-modified CNFs films fitted with the non-linear forms of Freundlich and Langmuir (left) and linear form of the Freundlich (right).

*5.2.3.3.Reusability of P4VP-PEO-modified CNFs films*

In terms of the reusability, Figure 25 indicates that TMPES and P4VP-PEO-modified CNFs films can be reused with negligible loss in adsorption capacity under the studied conditions. In fact, a small increase in the adsorption capacity can be appreciated after several cycles. This phenomenon can be related to the swelling of the CNFs fibers due to the high concentration of ethanol (95%) used to elude SMX [143]. Presumably, this swelling caused that P4VP-PEO molecules that were initially inaccessible to be exposed; therefore, they became available as new active sites for SMX adsorption. Moreover, a FTIR

analysis of films after adsorption and elution with ethanol did not show any measurable presence of SMX (Figure 26). This result suggests that SMX is almost completely removed from the surface of the films using this method.

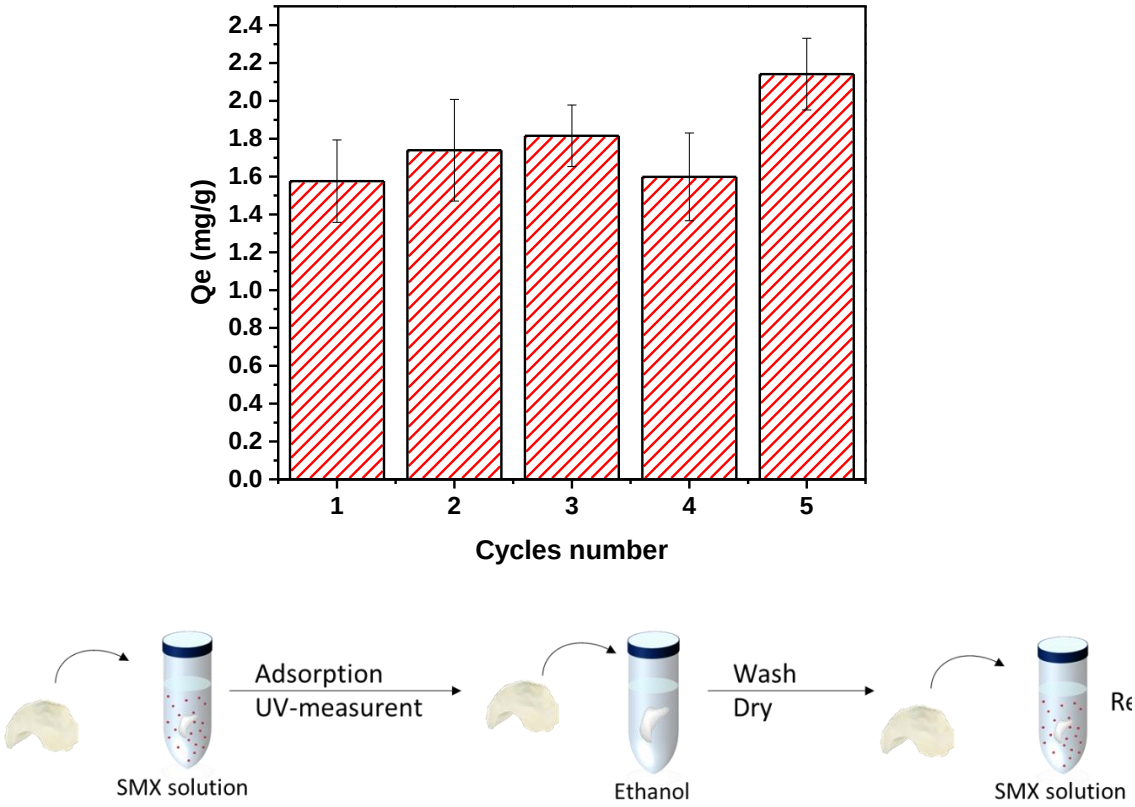


**Figure 26**. Adsorption capacity of TMPES and P4VP-PEO-modified CNFs films after different adsorption cycles of 25 ppm SMX for 1h equilibrium time (top). Schematic of the reusability process of the modified films (bottom).

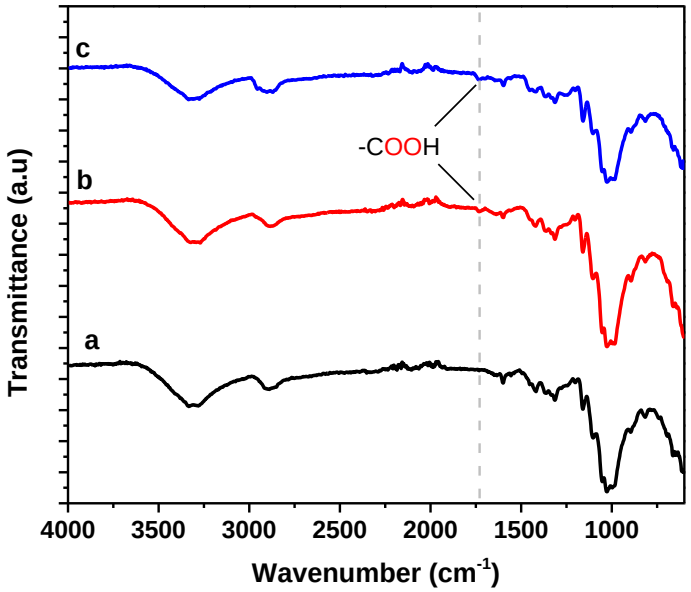


**Figure 27.** FTIR spectra of TMPES and P4VP-PEO-modified CNFs film after synthesis (unused) (a), after 3 reusability cycles in water (control) (b), and after 3 reusability cycle in 25 ppm SMX solutions (c).

## 5.3.Conclusions

A novel composite film was prepared by the modification of readily available and ecofriendly CNFs to adsorb SMX and, potentially, any pollutant with electron deficient aromatic structures. The modification of CNFs with the silane TMPES was critical to obtain a cellulose-based material that otherwise would be unstable in aqueous solution. The block copolymer P4VP-PEO dispersed in the surface of the films proved to be suitable for adsorbing SMX by means of EDA interactions. Interestingly, this type of interactions can allow a simple release of the adsorbed contaminant by elution with ethanol; consequently, it is possible to reuse the films. Characterization of the material showed that the films consist of CNFs fibers tightly accommodated in layers. This likely translates to adsorption active sites that are mostly available on the surface of the films. In addition to this, the morphology of the films could limit the diffusion of SMX during the adsorption process.

This could explain why the films reached the maximum adsorption capacity at short equilibration times. Fitting the adsorption isotherm with the Freundlich mathematical model suggests that the adsorption on the surface of the films is not homogeneous, and this could be directly related to distribution of the available P4VP-PEO. More interestingly, these films demonstrated to be reusable after several cycles without losing their adsorption capacity. Overall, the chemical characteristics and adsorptive behavior obtained with the studied films will positively contribute to the development of competitive materials for possible large-scale water remediation of EOCs.

CHAPTER SIX

# 6. PREPARATION OF POROUS MESH-REINFORCED CELLULOSE TRI-ACETATE MEMBRANES WITH AN EMBEDDED ACTIVE POLYMER.

## 6.1.Introduction

Among the strategies used to remove EOCs from wastewater and drinking water, processes that involve the use of membranes are considered the most effective [20]. Membrane processes such as forward osmosis (FO) and reverse osmosis (RO) have been extensively studied for rejection of EOCs [21-26]. Although there are several commercially available FO and RO systems, cellulose tri-acetate (CTA) has been the chosen material for the fabrication of those type of membranes due to its low-cost, availability, durability and non-toxicity [144, 145]. These membranes are commonly prepared by non-solvent induced phase separation (NIPS), where the polymer matrix (CTA) is dissolved in a solvent or mixture of solvents. The membrane is formed by coagulation in a non-solvent bath (generally water). This process leads to the formation of internal pores that allow the permeation of water while rejecting the contaminant molecule [145]. In the specific case of EOCs, degree of rejection depends greatly on the solute-membrane interactions such as steric exclusion, electrostatic and adsorptive interactions. These interactions will vary in terms of the physicochemical properties of the contaminant molecules being rejected [58]. However, as stated by Jin *et al*, since most EOCs are hydrophobic, the increasing affinity of those molecules with a membrane (adsorptive interactions), translates to higher rejection efficiencies [146]. Taking into consideration this finding, modification of CTA membranes with additives that promote the adsorption of EOCs could improve their rejection efficiency. competitive candidates to fulfill this task are block copolymers (BCPs). BCPs

are known for their variety in terms of physicochemical characteristic that are triggered by different chemical and conformational functionalities [121, 122]. BCPs can be fabricated from hydrophobic and hydrophilic monomers, that allows the variation of their conformation in response to external stimulus such as pH, solvent, temperature, etc. [63]. Ren *et al.* fabricated BCPs consisting of variable amount of 4-vinylpyridine (P4VP) and ethylene oxide (PEO) [132]. Analysis of the turbidity of the polymer solutions showed that these BCPs sharply respond to temperature and pH. This behavior was explained in terms of the PEO content and protonation/deprotonation of pyridine ring, respectively that change the structural conformation of the BCP in the solution. On the other hand, Li *et al.* exploited the pH-responsive characteristics of poly(methyl methacrylate -b- 4-vinylpyridine) PMMA-b-P4VP for the fabrication of membranes for the switchable adsorption of hydrophobic contaminants [140]. In that case, switchable characteristics of the membranes were achieved by the exposition of the hydrophobic P4VP polymer chains or the hydrophilic PMMA polymer chains. In that process membranes were able to drastically change their wettability behavior toward water or oils.

Taking into consideration the versatility of BCPs, it is possible to provide new and improved properties to CTA membranes with the addition of BCPs. Firstly, the presence of BCPs during the preparation of membranes using NIPS process could be determinant to their porosity. This is expected as additives are related to the formation, amount, shape and structure of pores in CTA membranes [147]. Secondly, the interactions with EOCs, and consequently their adsorption could also be improved by the functionalities of the BCPs used as additive. Among those interactions, addition of block copolymers that promotes adsorption based on electron-donor acceptor (EDA) or π-π are desirable since these type

of interactions are enough to achieve the adsorption, but can be reversed by external stimulus [148]. Following this idea, the modification of CTA membranes with appropriate BCPs could be reliable since most of EOCs coming from pharmaceutical activities are hydrophobic in nature and contain aromatic functionalities [2].

Here, it is presented the preparation of porous CTA membranes embedded with the block copolymer poly(4-vinylpyridine-b-ethylene oxide) (P4VP-PEO) by NIPS technique. These membranes were used for the adsorption of sulfamethoxazole (SMX), sulfadiazine (SDZ), and omeprazole (OMZ) as model EOCs. P4VP-PEO present in the membrane structure not only allowed the selective adsorption of EOCs by means of EDA interaction but resulted in higher surface area of the membranes. Adsorption and kinetic were evaluated through mathematical models such as Langmuir, Freundlich, pseudo- first and second orders. Adsorption of EOCs with those membranes proved to be reversible since the EDA interactions could be counteracted by simple solvent wash. In consequence, membranes could be reused for several adsorption cycles.

## 6.2.Results and Discussion

### 6.2.1. Modification of CTA membranes with P4VP-PEO

Cellulose triacetate (CTA) is well known due to its versatility and variability for the preparation of porous membranes and fibers for reverse and forward osmosis [149-152]. Here, characteristic such as the surface area and durability of CTA were exploited to create membranes modified with an adsorption active polymer. CTA used in this work has 39.8% wt acetyl substitution, this degree of acetylation is suitable for the preparation of the membranes by NIPS as reported elsewhere [26]. Moreover, As showed in Figure 27a,

several hydroxyl groups are available in the structure, meaning that this material could have a good wettability behavior. Since the membranes are intended for the selective adsorption of EOCs with low electron density, P4VP-PEO was selected as an additive for NIPS process. The high electron density of the pyridyl ring in the P4VP (Figure 27b) is capable of forming electron donor-acceptor (EDA) interactions with electron deficient regions in EOCs of interest [132]. The computer-generated electron density maps in Figure 28a show the electron deficient regions (green-blue) in SMX, SDZ, and OMZ. These regions are more susceptible to interact with P4VP-PEO by EDA [133]. Figure 28b shows a schematic of the EDA interaction between SMX and P4VP-PEO making emphasis in the reversibility caused by the addition of ethanol as a solvent.

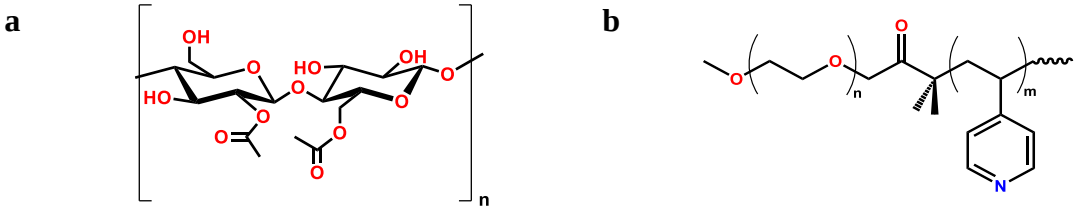


**Figure 28.** Molecular **s**tructures of (a) P4VP-PEO and (b) cellulose triacetate (CTA).

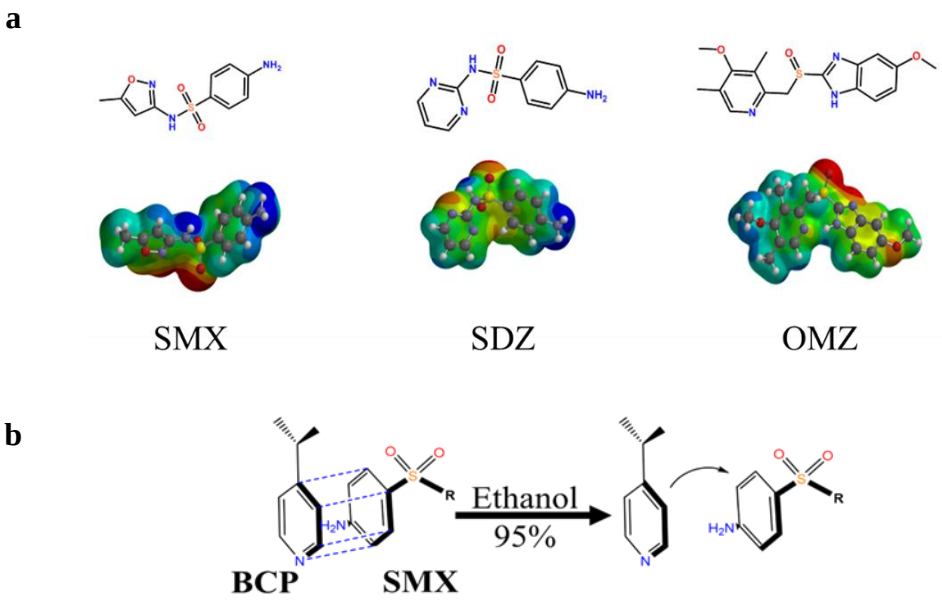


**Figure 29.** (a) Molecular structures of sulfamethoxazole (SMX), Sulfadiazine (SDZ), and omeprazole (OMZ). (b) Schematic of the adsorption-desorption of SMX using P4VP-PEO.

### 6.2.2. Characterization of CTA and CTA-P4VP-PEO membranes

FTIR was used to identify the functional groups corresponding to the different components of CTA membranes and CTA membranes modified with P4VP-PEO. Figure 29 shows the FTIR spectra of CTA membranes. At around 1730 $cm^{-1}$, there is a band corresponding to the stretching of the carbonyl of the acetyl group. The band at 1370 $cm^{-1}$ corresponds to the bending vibration of methylene groups (-$CH_2$). The intense band at 1217 $cm^{-1}$ corresponds to the (-C-O) stretching vibration, while a sharp band around 1030 $cm^{-1}$ corresponds to the glycosidic ring stretching[153]. Despite of FTIR spectrum of CTA membrane modified with P4VP-PEO apparently do not differ from that of the CTA membrane without modification, a close inspection reveals a new band at 1596 $cm^{-1}$ (inset of spectra). This bands corresponds to vibrations of the pyridine ring that are also present in the spectrum of P4VP-PEO [138]. It is worth mentioning that the low intensity of that

band was expected since the FTIR-ATR method used only analyzes the surface of the material while P4VP-PEO is embedded inside the membrane structure.

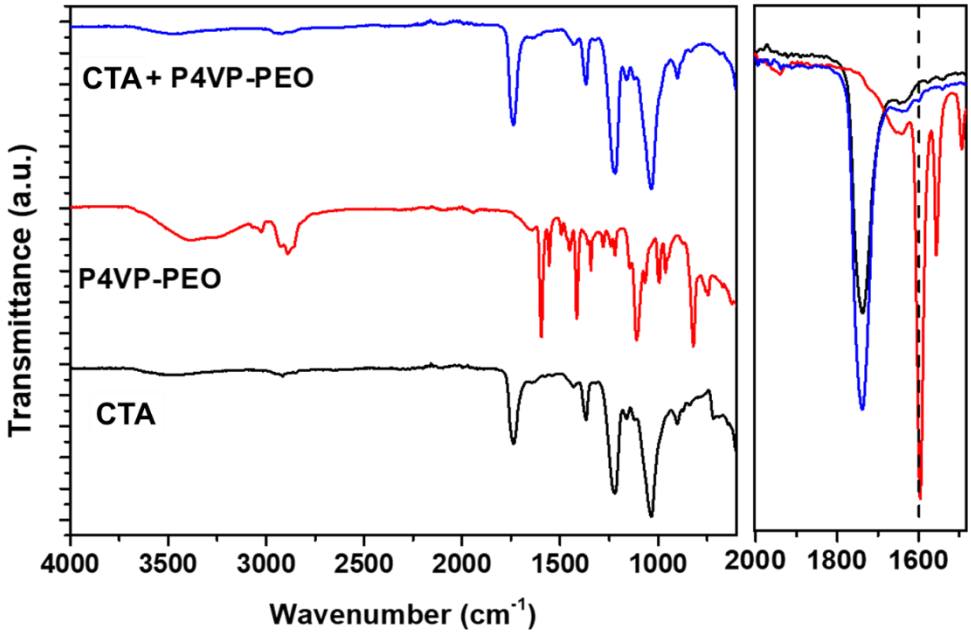


**Figure 30.** FTIR spectra of CTA membrane, P4VP-PEO and CTA membrane modified with P4VP-PEO.

SEM was used to characterize the surface and internal morphology (cross-section) of CTA membranes. When CTA membranes without P4VP-PEO where analyzed, it was noted that the front and back side presented a smooth surface with minor deformations (Figure 30a and 30b, respectively). However, the cross-section of the membrane (Figure 30c) showed a large number of pores which are formed due to the nucleation process during the phase separation [154]. Even though the presence of pores was confirmed, no apparent connection or channels between the pores was detected in the top and back surfaces of the membrane. On the other hand, CTA membranes modified with P4VP-PEO presented small pores in the front side and large pores in the back side (Figure 30d and 30e, respectively).

More interestingly, the cross-section (Figure 30f) showed hierarchical pores that connected both side of the membrane. This behavior can only be explained by the presence of P4VP-PEO. During the phase separation, the hydrophobic ethylene oxide chains of the BCP allow a higher water (non-solvent) penetration in the CTA matrix, changing the overall nucleation effect.

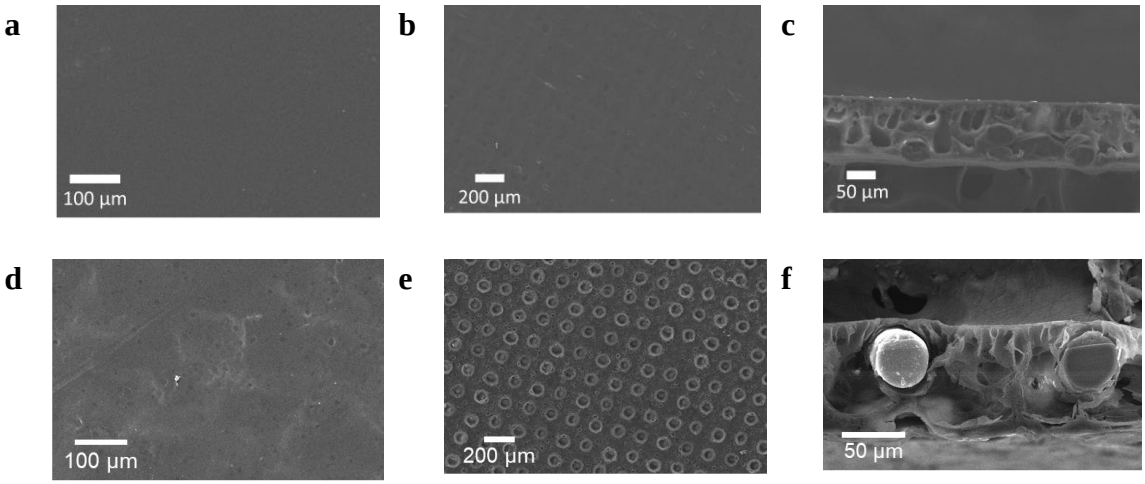


**Figure 31.** SEM micrographs of (a) front side, (b) back side and (c) cross-section of CTA membranes. SEM micrographs of (d) front side, (e) back side and (f) cross section of CTA membranes modified with P4VP-PEO.

Contact angle measurements were used to estimate the wettability of CTA membranes and CTA membranes modified with P4VP-PEO. Taking into consideration that CTA used in this study has a 39.8% wt. substitution, membranes with considerable wettability were expected. In this case, the contact angle was 60º at time 0 s (Figure 31a). After 120 s, the value decreased to 50º due to the water penetration, a process mediated by diffusion through the membrane. When CTA membranes modified with P4VP-PEO were tested (Figure 31b), a similar result was obtained (contact angle of 60 º) since P4VP-PEO would not change the hydrophilicity/hydrophobicity of the membrane. However, after 120 s, there is no apparent change in the contact angle. This phenomenon can be tentatively attributed

to the porosity of the membrane. These pores are filled with air molecules that are hydrophobic and reduce the penetration of the water into the membrane structure.

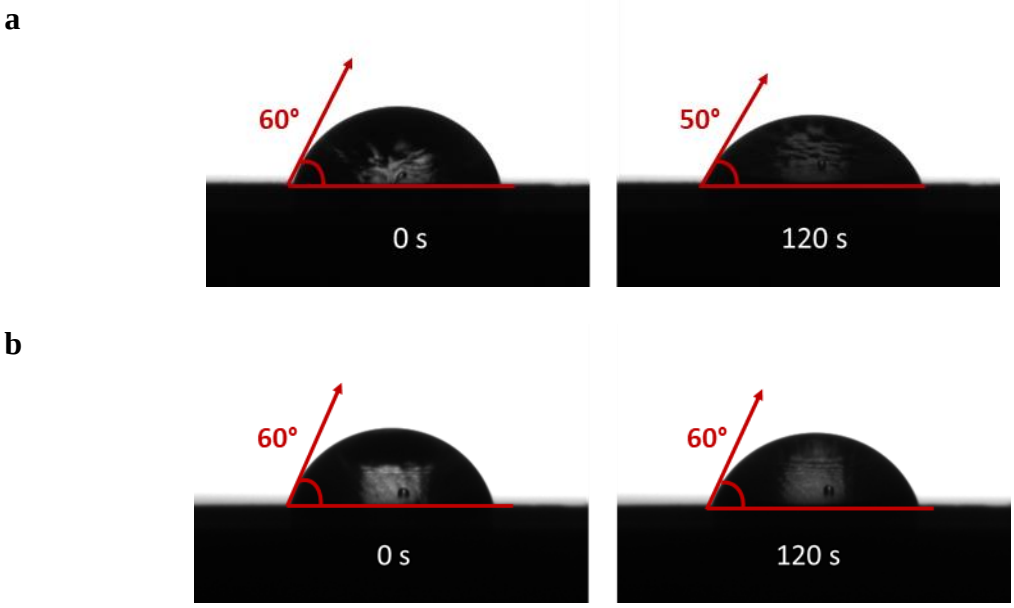


**Figure 32.** Contact angle measurements of a) CTA membranes, b) CTA membranes modified with P4VP-PEO.

### 6.2.3. Adsorption batch tests of SMX, SDZ and OMZ using CTA membranes

Adsorption batch tests were performed in order to assess the adsorption capability of CTA membranes and CTA membranes modified with P4VP-PEO against SMX, SDZ, and OMZ as model EOCs compounds. These tests include adsorption analysis as a function of time, adsorption isotherms and reusability. Figure 32 shows a comparison of preliminary equilibrium adsorption amount of SMX, OMZ, and SDZ using CTA membranes and CTA-P4VP-PEO membranes. In all cases, it is evident the increase of the equilibrium adsorption amount when P4VP-PEO is embedded in the membrane. Adsorption of SMX was highly enhanced by the presence of P4VP-PEO, with lesser extent for OMZ and SDZ, respectively. Since batch adsorption conditions were the same for the three EOCs,

differences in the improved $q_e$ can be attributed to the interaction of each compound with P4VP-PEO. For SMX, the phenyl group of this molecule has a higher π electron delocalization due to the sulfo and heterocyclic groups that make EDA interactions more effective. In addition, pkas of SMX (1.4 and 5.8) lead to a negative species at neutral pH, promoting further interaction with the ethylene oxide chains of P4VP-PEO [155]. Adsorption of OMZ with modified membranes can be addressed in terms of the functional groups in its structure. In one hand, it has two ether functionalities that behave like electron-withdrawing groups. However, the pyridine and imidazole groups are electron-donor, meaning that the net π electron deficiency of OMZ is not as high as in SMX, thus explaining its lower adsorption [156]. Adsorption of SDZ, on the other hand, is the opposite of that of the SMX. Here, the nitrogen groups provide appropriate electron density to the electron-withdrawing sulfo group, making the molecule neutral in term of EDA interactions with P4VP-PEO. In addition, at the studied pH, this molecule has no net charge, which further decreases the interaction with the BCP or the CTA matrix [157].

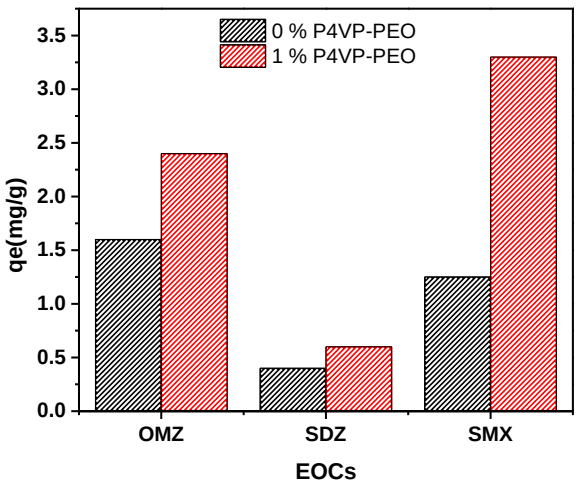


**Figure 33.** Comparative bar plot of the adsorption capacities (*qe*) obtained for each EOC with CTA and modified CTA membranes.

A simple inspection of Figure 32 could suggest that the adsorption of SDZ or OMZ is not remarkable. However, it is worth mentioning that $q_e$ calculation takes into consideration the mass of the membrane, including the polyester mesh used as a reinforcement. This material account for nearly 50% of the mass of the membrane and do not contribute to its adsorption capability. Moreover, the mass contribution to the actual membrane is approximately 5.8%, meaning that a small amount of P4VP-PEO is enough to significantly increase the adsorption capacity of the CTA membrane, particularly when SMX is considered. These results will be complemented by later discussion addressing the adsorption mechanisms of EOCs with the membrane.

*6.2.3.1.Adsorption as a function of time*

Figure 33 shows the adsorption kinetics of SMX, OMZ, and SDZ by modified CTA membranes at an initial concentration of 30 ppm. All EOCs are initially adsorbed very fast until reaching a plateau. This phenomenon is related to large mass transfer of the solute to the membrane surface, followed by slow adsorption until reaching equilibrium. At that point, EOCs start to slowly penetrate the inner pores of the membrane [157]. Kinetic analysis of these adsorption data was performed using the nonlinear fitting of pseudo-first and pseudo-second order models [158, 159]. The following equations describe the mathematical forms of both models.

$$q_t = q_e(1 - \exp(-k_1 t)) \qquad 6$$

$$q_t = \frac{k_2 q_e^2 t}{1 + k_2 q_e t} \quad (7)$$

Where $q_e$ and $q_t$ are adsorption amount at equilibrium and time ($t$), respectively. $k_1$ is the rate constant of pseudo-first order adsorption, and $k_2$ is the equilibrium rate constant of pseudo-second order adsorption. In all EOC adsorption cases, the $R^2$ for pseudo-second order adsorption was higher of those of the pseudo-second order adsorptions. These results suggest that the adsorption mechanism of EOCs on the modified CTA membranes is mostly related to chemical interactions or chemisorptions where there is an exchange or sharing of electrons between EOCs and the modified membranes [160]. This model is in good agreement with the characteristic of EDA interactions expected for the electron donor pyridine group of P4VP-PEO and the electron-deficient aromatic groups of the EOCs.

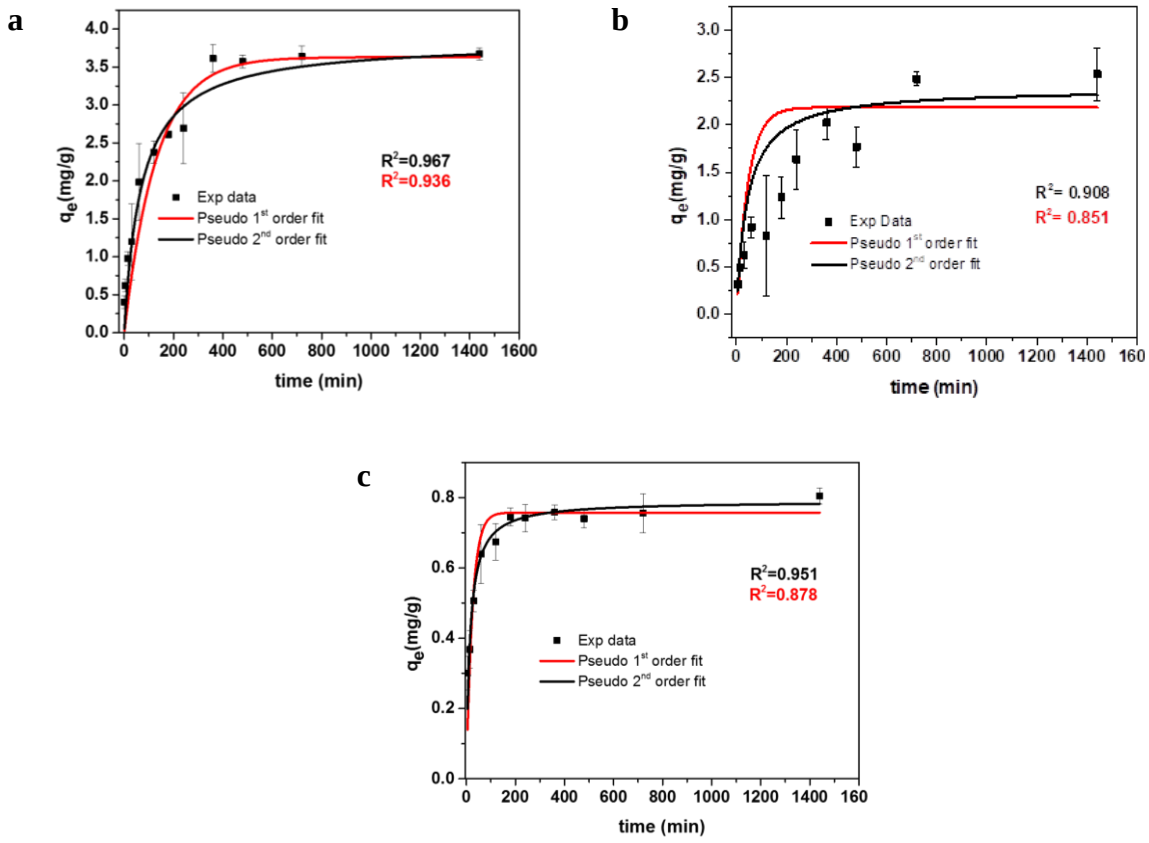


**Figure 34.** Effect of the contact time on the adsorption of a) SMX, b) OMZ, and c) SDZ. Each graph was fitted with the nonlinear forms of pseudo -first and second models.

### *6.2.3.2.Adsorption isotherm experiments*

Figure 34 shows the adsorption equilibrium isotherms of the three EOCs on CTA membranes modified with P4VP-PEO. These plots provide a good idea of how the concentration of the EOC affects the adsorption capability of the membranes. In all the cases, the adsorption of the EOCs increases proportionally to their concentration. However, a plateau is expected a higher concentration since the adsorbent material is not able to accommodate further solute. Here, the concentration tested in the study was not high enough for that to occur, meaning that the full capacity of the membranes was not achieved. A close inspection of the plots reveals that the adsorption has a slight tendency to the

expected plateau. To further analyze the adsorption isotherm data, mathematical models of Freundlich and Langmuir were performed. Freundlich approach assumes the formation of multilayers of adsorption with a heterogeneous or non-uniform distribution of the adsorption active sites along the surface of the adsorbant [141]. The mathematical form of this model uses the equation 4.

Langmuir model assumes that the solute forms a homogeneous monolayer on the surface of the adsorbent and governed by the following equation [141]:

$$\frac{C_e}{q_e} = \frac{C_e}{q_m} + \frac{1}{K_L q_m} \qquad 8$$

Where $q_m$ is the theoretically maximum adsorption amount and $K_L$ is the Langmuir constant. Nonlinear fitting of both models is presented in Figure 34 with their respective $R^2$ values. With the exception of SMX, the Freundlich model was in good agreement with the adsorption isotherms of OMZ and SDZ, which suggests the heterogeneous distribution of the contaminants in the structure of the membrane. The case of SMX is different in terms of the behavior of the actual adsorption curve. This curve seems to be composed of two consecutive steps that avoid any fitting with the two models. This behavior could be interpreted as a possible breakthrough of the membrane in response to the increasing concentration of the SMX in the solution [161, 162].

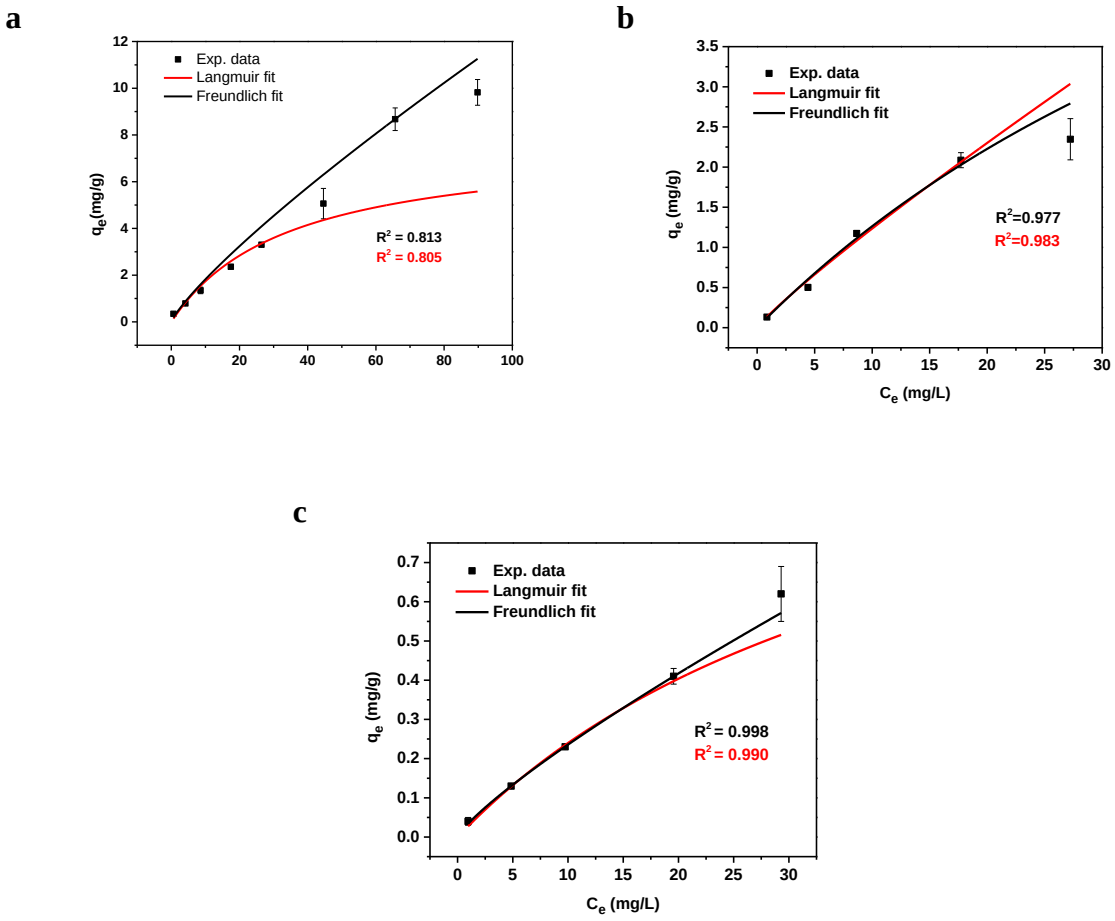


**Figure 35.** Adsorption istherms plots of a) SMZ, b) OMZ, and c) SDZ with their respective nonlinear fitting of Langmuir and Freundlich mathematical models.

### *6.2.3.3.Reusability of the membranes*

Reusability of adsorbent materials is as important as its adsorption capacity. When designing the membranes, cost-effectiveness played a significant role in this study. It was established before in this study the availability of CTA, as well as the small amount of P4VP-PEO needed for the preparation of the membrane. In addition, NIPS is a well-known method for the development of membrane [163]. Now, as showed in Figure 35, the reusability of the CTA modified with P4VP-PEO presented promising results since successive adsorption cycles of the three EOCs prove to be successful. In fact, in the case

of OMZ and SDZ, it can seem an increase in the adsorption capacity after the second cycle. This phenomenon could be related to the possibility of the formation of new non-specific interactions with the membrane after every elution process. The later behavior does not seem to be the case of the different adsorption cycles of SMX. In this case, there is a very consistent adsorption capacity retention, which suggests that the EDA interaction SMX-P4VP-PEO are fully reversible. It is worth to mention that minor degradation of the membrane could occur after each wash cycle (elution), but it does not seem to be affecting the efficiency of the modified CTA membrane.

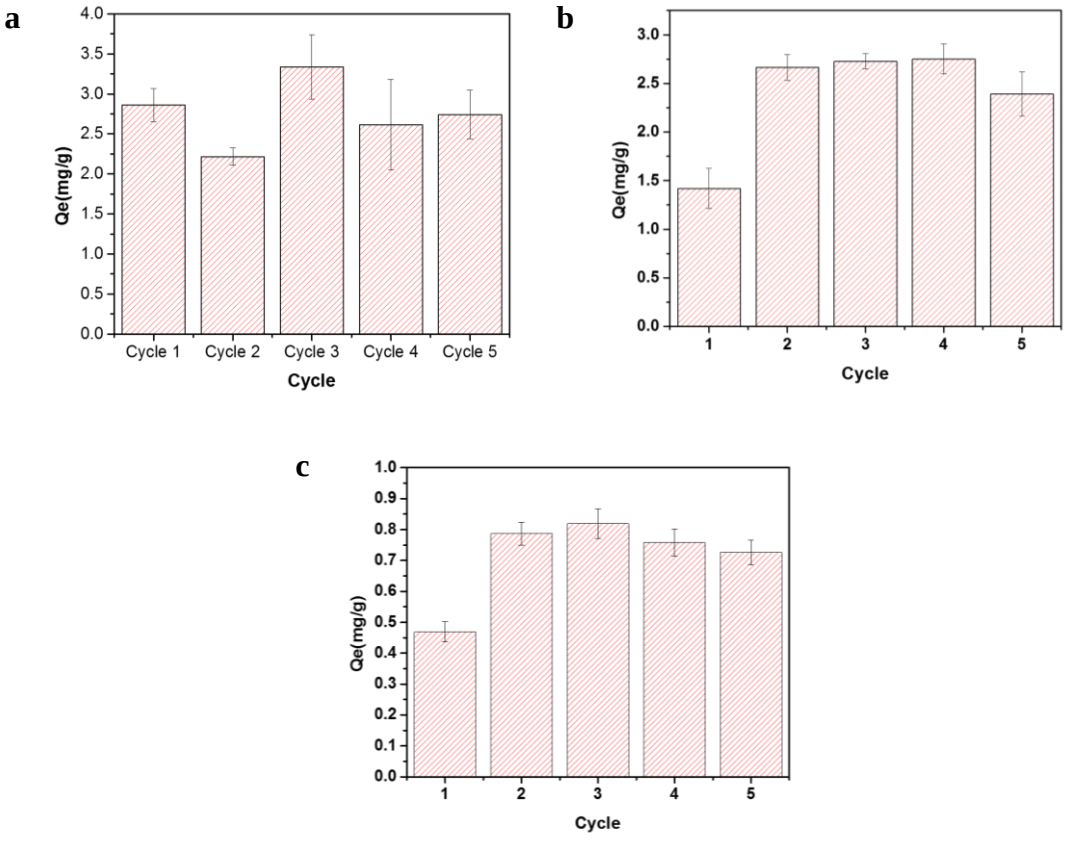


**Figure 36.** Adsorption capacity of a)SMX, b) OMZ, and c) SDZ after several cycles of adsorption with CTA membranes modiffied with P4VP-PEO.

## 6.3.Conclusions

Porous CTA membranes embedded with P4VP-PEO were successfully prepared using low-cost NIPS for the adsorption of EOCs. A comprehensive analysis presented in this study proved that these membranes not only have the porosity and stability required for the adsorption of contaminants but are cost-effective and reusable. P4VP-PEO used for the modification of the membrane demonstrated to be a complete synergistic additive. During the NIPS process, it allowed the formation of hierarchical pores in the membrane due to the increased nucleation caused by its enhanced hydrophilicity. Also, the BCP structural and chemical characteristics were essential for selective and reversible adsorption to electron-deficient aromatic compounds such as SMX. The selective adsorption features of the modified membranes were systematically demonstrated for less electron-deficient compounds such as OMZ and SDZ. Moreover, only a small amount of this BCP was necessary to increase the adsorption capacity of the membranes significantly. Overall results of this study translate into an efficient, low-cost, and eco-friendly method to produce selective and reusable adsorption membranes that contribute to further development of large-scale EOCs remediation applications.

CHAPTER SEVEN

# 7. GENERAL CONCLUSIONS

In this research, it was demonstrated the feasibility of the adsorption of EOCs using the environmental-friendly cellulose derivates in combination with BCP. This finding comes from the evaluation of different cellulose-BCP composite structures, named nanocrystals, nanofibers films, and porous membranes. Adsorption evaluation using nanocrystals gave us a good understanding of how the contaminants interact with a specific adsorbent at the molecular level. In that case, the modification of just the surface of the nanocrystals was key for the theoretical evaluation. The computational calculations resulted in binding energies of 21.2 kcal/mol, 14.3 kcal/mol and 8.4 kcal/mol for ACE, SMX, and DEET, respectively, related to hydrogen bonds and/or van der Waals interactions with the polymer chain. Moving to the experimental adsorption procedure, it was determined that the dispersion of the material could be problematic at the moment of the execution of desorption-reusability assays. For that reason, it was evaluated the fabrication of CNFs films modified with a BCP with a chemical functionality suitable for the EDA interactions with EOCs. In this case, modification of CNFs with the silane TMPES was critical to obtain a cellulose-based material stable in aqueous solution. This modification constituted a considerable improvement with respect of the nanocrystal approach for the adsorption of the EOCs. In addition, results suggested that the BCP, P4VP-PEO, was the significant player when the interaction with the EOC is considered. More interestingly, these films demonstrated to be reusable after several cycles without losing their adsorption capacity.

Knowing the promising capabilities of P4VP-PEO in terms of the adsorption of EOCs, a new study involving the modification of CTA porous membranes with this BCP was conducted. A comprehensive analysis presented in this study proved that these membranes not only have the porosity and stability required for the adsorption of contaminants but are cost-effective and reusable. P4VP-PEO used for the modification of the membrane demonstrated to be a complete synergistic additive. During the NIPS process, it allowed the formation of hierarchical pores in the membrane due to the increased nucleation caused by its enhanced hydrophilicity. Adsorption evaluation of the membranes was very rewarding since those results were in good agreement with the adsorption characteristic of P4VP-PEO. More specifically, the selective properties of the electron-donor pyridine toward electron-deficient aromatic compounds. Moreover, only a small amount of P4VP-PEO was necessary to increase the adsorption capacity of the membranes significantly. Overall results of this study translate into an efficient, low-cost, and eco-friendly method to produce selective and reusable adsorption membranes that contribute to further development of large-scale EOCs remediation applications.

# 8. REFERENCES

[1] J. Rivera-Utrilla, M. Sanchez-Polo, M.A. Ferro-Garcia, G. Prados-Joya, R. Ocampo-Perez, Pharmaceuticals as emerging contaminants and their removal from water. A review, Chemosphere, 93 (2013) 1268-1287.

[2] P.E. Stackelberg, E.T. Furlong, M.T. Meyer, S.D. Zaugg, A.K. Henderson, D.B. Reissman, Persistence of pharmaceutical compounds and other organic wastewater contaminants in a conventional drinking-water-treatment plant, Sci. Total Environ., 329 (2004) 99-113.

[3] M.A. Marcoux, M. Matias, F. Olivier, G. Keck, Review and prospect of emerging contaminants in waste – Key issues and challenges linked to their presence in waste treatment schemes: General aspects and focus on nanoparticles, Waste Manage., 33 (2013) 2147-2156.

[4] D. Dolar, M. Gros, S. Rodriguez-Mozaz, J. Moreno, J. Comas, I. Rodriguez-Roda, D. Barcelo, Removal of emerging contaminants from municipal wastewater with an integrated membrane system, MBR-RO, J. Hazard. Mater., 239-240 (2012) 64-69.

[5] A. Rossner, S.A. Snyder, D.R. Knappe, Removal of emerging contaminants of concern by alternative adsorbents, Water. Res., 43 (2009) 3787-3796.

[6] S.D. Richardson, Environmental mass spectrometry: emerging contaminants and current issues, Anal. Chem., 84 (2012) 747-778.

[7] B. Kunst, K. Košutić, Removal of Emerging Contaminants in Water Treatment by Nanofiltration and Reverse Osmosis, in: D. Barceló, M. Petrovic (Eds.) Emerging Contaminants from Industrial and Municipal Waste: Removal Technologies, Springer Berlin Heidelberg, Berlin, Heidelberg, 2008, pp. 103-125.

[8] M.F. Secondes, V. Naddeo, V. Belgiorno, F. Ballesteros, Jr., Removal of emerging contaminants by simultaneous application of membrane ultrafiltration, activated carbon adsorption, and ultrasound irradiation, J. Hazard. Mater., 264 (2014) 342-349.

[9] P.C. Mouli, S.V. Mohan, S.J. Reddy, Electrochemical processes for the remediation of wastewater and contaminated soil: emerging technology, J. Sci. Ind. Res., 63 (2004) 11-19.

[10] S.A. Snyder, S. Adham, A.M. Redding, F.S. Cannon, J. DeCarolis, J. Oppenheimer, E.C. Wert, Y. Yoon, Role of membranes and activated carbon in the removal of endocrine disruptors and pharmaceuticals, Desalination, 202 (2007) 156-181.

[11] A. Pal, K.Y.-H. Gin, A.Y.-C. Lin, M. Reinhard, Impacts of emerging organic contaminants on freshwater resources: Review of recent occurrences, sources, fate and effects, Sci. Total Environ., 408 (2010) 6062-6069.

[12] C. Sichel, C. Garcia, K. Andre, Feasibility studies: UV/chlorine advanced oxidation treatment for the removal of emerging contaminants, Water Res., 45 (2011) 6371-6380.

[13] K. Ikehata, M. Gamal El-Din, S.A. Snyder, Ozonation and Advanced Oxidation Treatment of Emerging Organic Pollutants in Water and Wastewater, Ozone-Sci. Eng., 30 (2008) 21-26.

[14] A. Papageorgiou, D. Voutsa, N. Papadakis, Occurrence and fate of ozonation by-products at a full-scale drinking water treatment plant, Sci. Total Environ., 481 (2014) 392-400.

[15] S.D. Richardson, Disinfection by-products and other emerging contaminants in drinking water, TrAC-Trend. Anal. Chem., 22 (2003) 666-684.

[16] S.D. Richardson, M.J. Plewa, E.D. Wagner, R. Schoeny, D.M. DeMarini, Occurrence, genotoxicity, and carcinogenicity of regulated and emerging disinfection by-products in drinking water: A review and roadmap for research, Mutat. Res.-Rev. Mutat., 636 (2007) 178-242.

[17] Z. Yu, S. Peldszus, P.M. Huck, Adsorption characteristics of selected pharmaceuticals and an endocrine disrupting compound—Naproxen, carbamazepine and nonylphenol—on activated carbon, Water Res., 42 (2008) 2873-2882.

[18] A. Ahmadpour, D.D. Do, The preparation of active carbons from coal by chemical and physical activation, Carbon, 34 (1996) 471-479.

[19] Y. Matsui, Y. Fukuda, T. Inoue, T. Matsushita, Effect of natural organic matter on powdered activated carbon adsorption of trace contaminants: characteristics and mechanism of competitive adsorption, Water Res., 37 (2003) 4413-4424.

[20] H. Andersen, H. Siegrist, B. Halling-Sørensen, T.A. Ternes, Fate of Estrogens in a Municipal Sewage Treatment Plant, Environ. Sci. & Technol., 37 (2003) 4021-4026.

[21] M.A. Al-Obaidi, J.P. Li, C. Kara-Zaïtri, I.M. Mujtaba, Optimisation of reverse osmosis based wastewater treatment system for the removal of chlorophenol using genetic algorithms, Chem. Eng. J., 316 (2017) 91-100.

[22] E. Steinle-Darling, M. Zedda, M.H. Plumlee, H.F. Ridgway, M. Reinhard, Evaluating the impacts of membrane type, coating, fouling, chemical properties and water chemistry on reverse osmosis rejection of seven nitrosoalklyamines, including NDMA, Water Res., 41 (2007) 3959-3967.

[23] D. Dolar, M. Gros, S. Rodriguez-Mozaz, J. Moreno, J. Comas, I. Rodriguez-Roda, D. Barceló, Removal of emerging contaminants from municipal wastewater with an integrated membrane system, MBR–RO, J. of Hazard. Mater., 239-240 (2012) 64-69.

[24] M. Xie, L.D. Nghiem, W.E. Price, M. Elimelech, Comparison of the removal of hydrophobic trace organic contaminants by forward osmosis and reverse osmosis, Water Res., 46 (2012) 2683-2692.

[25] A. D'Haese, P. Le-Clech, S. Van Nevel, K. Verbeken, E.R. Cornelissen, S.J. Khan, A.R.D. Verliefde, Trace organic solutes in closed-loop forward osmosis applications: Influence of membrane fouling and modeling of solute build-up, Water Res., 47 (2013) 5232-5244.

[26] T.P.N. Nguyen, E.-T. Yun, I.-C. Kim, Y.-N. Kwon, Preparation of cellulose triacetate/cellulose acetate (CTA/CA)-based membranes for forward osmosis, J. Membrane Sci., 433 (2013) 49-59.

[27] F.S. Bates, G.H. Fredrickson, Block Copolymers—Designer Soft Materials, Phys. Today, 52 (1999) 32.

[28] F.S. Bates, M.A. Hillmyer, T.P. Lodge, C.M. Bates, K.T. Delaney, G.H. Fredrickson, Multiblock polymers: panacea or Pandora's box?, Science, 336 (2012) 434-440.

[29] M.W. Matsen, M. Schick, Stable and unstable phases of a diblock copolymer melt, Phys. Rev. Lett., 72 (1994) 2660-2663.

[30] S.D. Richardson, T.A. Ternes, Water Analysis: Emerging Contaminants and Current Issues, Anal. Chem., 90 (2018) 398-428.

[31] S.D. Richardson, T.A. Ternes, Water Analysis: Emerging Contaminants and Current Issues, Anal. Chem., 83 (2011) 4614-4648.

[32] M. Petrovic, D. Barceló, Application of liquid chromatography/quadrupole time-of-flight mass spectrometry (LC-QqTOF-MS) in the environmental analysis, J. Mass Spectrom., 41 (2006) 1259-1267.

[33] J.M. Diamond, H.A. Latimer Ii, K.R. Munkittrick, K.W. Thornton, S.M. Bartell, K.A. Kidd, Prioritizing contaminants of emerging concern for ecological screening assessments, Environ. Toxicol. Chem., 30 (2011) 2385-2394.

[34] L.J. Guillette, Jr., Endocrine disrupting contaminants--beyond the dogma, Environ Health Perspect, 114 Suppl 1 (2006) 9-12.

[35] S. Milla, S. Depiereux, P. Kestemont, The effects of estrogenic and androgenic endocrine disruptors on the immune system of fish: a review, Ecotoxicology, 20 (2011) 305-319.

[36] W. Mnif, A.I.H. Hassine, A. Bouaziz, A. Bartegi, O. Thomas, B. Roig, Effect of Endocrine Disruptor Pesticides: A Review, Int. J. Env. Res. Pub. He., 8 (2011) 2265-2303.

[37] A.C. Gore, Developmental programming and endocrine disruptor effects on reproductive neuroendocrine systems, Front. Neuroendocrin., 29 (2008) 358-374.

[38] D.S. Chormey, Ç. Büyükpınar, F. Turak, O.T. Komesli, S. Bakırdere, Simultaneous determination of selected hormones, endocrine disruptor compounds, and pesticides in water medium at trace levels by GC-MS after dispersive liquid-liquid microextraction, Environ. Monit. Assess., 189 (2017) 277.

[39] N. Bolong, A.F. Ismail, M.R. Salim, T. Matsuura, A review of the effects of emerging contaminants in wastewater and options for their removal, Desalination, 239 (2009) 229-246.

[40] P.a.S.P. Division, 305(b)/303(d) Integrated Report, in, Puerto Rico Environmental Quality Board, San Juan, Puerto Rico, 2013, pp. 113-117.

[41] A. Melo-Guimarães, F.J. Torner-Morales, J.C. Durán-Álvarez, B.E. Jiménez-Cisneros, Removal and fate of emerging contaminants combining biological, flocculation and membrane treatments, Water Sci. Technol., 67 (2013) 877-885.

[42] M. Carballa, F. Omil, J.M. Lema, M.a. Llompart, C. García-Jares, I. Rodríguez, M. Gómez, T. Ternes, Behavior of pharmaceuticals, cosmetics and hormones in a sewage treatment plant, Water Res., 38 (2004) 2918-2926.

[43] K.E. Pinkston, D.L. Sedlak, Transformation of Aromatic Ether- and Amine-Containing Pharmaceuticals during Chlorine Disinfection, Environ. Sci. Technol., 38 (2004) 4019-4025.

[44] F.J. Benitez, J.L. Acero, F.J. Real, G. Roldan, E. Rodriguez, Photolysis of model emerging contaminants in ultra-pure water: Kinetics, by-products formation and degradation pathways, Water Res., 47 (2013) 870-880.

[45] B. Guo, L. Chang, K. Xie, Adsorption of Carbon Dioxide on Activated Carbon, J. Nat. Gas Chem., 15 (2006) 223-229.

[46] M.F.N. Secondes, V. Naddeo, V. Belgiorno, F. Ballesteros, Removal of emerging contaminants by simultaneous application of membrane ultrafiltration, activated carbon adsorption, and ultrasound irradiation, J. Hazard. Mater., 264 (2014) 342-349.

[47] A. Katsigiannis, C. Noutsopoulos, J. Mantziaras, M. Gioldasi, Removal of emerging pollutants through Granular Activated Carbon, Chem. Eng. J., 280 (2015) 49-57.

[48] S.Á. Torrellas, R. García Lovera, N. Escalona, C. Sepúlveda, J.L. Sotelo, J. García, Chemical-activated carbons from peach stones for the adsorption of emerging contaminants in aqueous solutions, Chem. Eng. J., 279 (2015) 788-798.

[49] L.F. Delgado, P. Charles, K. Glucina, C. Morlay, Adsorption of Ibuprofen and Atenolol at Trace Concentration on Activated Carbon, Sep. Sci. Technol., 50 (2015) 1487-1496.

[50] M. Franz, H.A. Arafat, N.G. Pinto, Effect of chemical surface heterogeneity on the adsorption mechanism of dissolved aromatics on activated carbon, Carbon, 38 (2000) 1807-1819.

[51] W.K. Lafi, Production of activated carbon from acorns and olive seeds, Biomass and Bioenergy, 20 (2001) 57-62.

[52] M. Açıkyıldız, A. Gürses, S. Karaca, Preparation and characterization of activated carbon from plant wastes with chemical activation, Micropor. Mesopor. Mat., 198 (2014) 45-49.

[53] E. Sabio, E. González, J.F. González, C.M. González-García, A. Ramiro, J. Gañan, Thermal regeneration of activated carbon saturated with p-nitrophenol, Carbon, 42 (2004) 2285-2293.

[54] B.D. Coday, B.G.M. Yaffe, P. Xu, T.Y. Cath, Rejection of Trace Organic Compounds by Forward Osmosis Membranes: A Literature Review, Environ. Sci. Technol., 48 (2014) 3612-3624.

[55] V. Yangali-Quintanilla, S.K. Maeng, T. Fujioka, M. Kennedy, Z. Li, G. Amy, Nanofiltration vs. reverse osmosis for the removal of emerging organic contaminants in water reuse, Desalin. Water Treat., 34 (2011) 50-56.

[56] J.L. Acero, F.J. Benitez, F.J. Real, F. Teva, Removal of emerging contaminants from secondary effluents by micellar-enhanced ultrafiltration, Sep. Purif. Technol., 181 (2017) 123-131.

[57] R. Valladares Linares, V. Yangali-Quintanilla, Z. Li, G. Amy, Rejection of micropollutants by clean and fouled forward osmosis membrane, Water Res., 45 (2011) 6737-6744.

[58] S. Kim, K.H. Chu, Y.A.J. Al-Hamadani, C.M. Park, M. Jang, D.-H. Kim, M. Yu, J. Heo, Y. Yoon, Removal of contaminants of emerging concern by membranes in water and wastewater: A review, Chem. Eng. J., 335 (2018) 896-914.

[59] B. Bhattarai, M. Muruganandham, R.P.S. Suri, Development of high efficiency silica coated β-cyclodextrin polymeric adsorbent for the removal of emerging contaminants of concern from water, J. Hazard. Mater., 273 (2014) 146-154.

[60] S. Kawano, T. Kida, K. Miyawaki, Y. Noguchi, E. Kato, T. Nakano, M. Akashi, Cyclodextrin Polymers as Highly Effective Adsorbents for Removal and Recovery of Polychlorobiphenyl (PCB) Contaminants in Insulating Oil, Environ. Sci. Technol., 48 (2014) 8094-8100.

[61] X. Qin, L. Bai, Y. Tan, L. Li, F. Song, Y. Wang, β-Cyclodextrin-crosslinked polymeric adsorbent for simultaneous removal and stepwise recovery of organic dyes and heavy metal ions: Fabrication, performance and mechanisms, Chem. Eng. J., 372 (2019) 1007-1018.

[62] Y. Patiño, E. Díaz, S. Ordóñez, E. Gallegos-Suarez, A. Guerrero-Ruiz, I. Rodríguez-Ramos, Adsorption of emerging pollutants on functionalized multiwall carbon nanotubes, Chemosphere, 136 (2015) 174-180.

[63] H. Otsuka, Y. Nagasaki, K. Kataoka, Self-assembly of block copolymers, Mater. Today, 4 (2001) 30-36.

[64] G. Gaucher, M.-H. Dufresne, V.P. Sant, N. Kang, D. Maysinger, J.-C. Leroux, Block copolymer micelles: preparation, characterization and application in drug delivery, J. Control. Release, 109 (2005) 169-188.

[65] K. Kataoka, A. Harada, Y. Nagasaki, Block copolymer micelles for drug delivery: Design, characterization and biological significance, Adv. Drug Deliver. Rev., 64 (2012) 37-48.

[66] V. Abetz, Isoporous block copolymer membranes, Macromol. Rapid. Commun., 36 (2015) 10-22.

[67] H. Strathmann, K. Kock, The formation mechanism of phase inversion membranes, Desalination, 21 (1977) 241-255.

[68] P. Vandezande, L.E. Gevers, I.F. Vankelecom, Solvent resistant nanofiltration: separating on a molecular level, Chem. Soc. Rev., 37 (2008) 365-405.

[69] C. Hörenz, C. Pietsch, A.S. Goldmann, C. Barner-Kowollik, F.H. Schacher, Phase Inversion Membranes from Amphiphilic Diblock Terpolymers, Adv. Mater. Inf., 2 (2015) 1500042.

[70] E.J. Vriezekolk, K. Nijmeijer, W.M. de Vos, Dry–wet phase inversion block copolymer membranes with a minimum evaporation step from NMP/THF mixtures, J. Membrane Sci., 504 (2016) 230-239.

[71] A. Dufresne, Nanocellulose: a new ageless bionanomaterial, Mater. Today, 16 (2013) 220-227.

[72] N. Lin, A. Dufresne, Nanocellulose in biomedicine: Current status and future prospect, Eur. Polym. J., 59 (2014) 302-325.

[73] N. Lin, A. Dufresne, Surface chemistry, morphological analysis and properties of cellulose nanocrystals with gradiented sulfation degrees, Nanoscale, 6 (2014) 5384-5393.

[74] H.A. Silvério, W.P. Flauzino Neto, D. Pasquini, Effect of Incorporating Cellulose Nanocrystals from Corncob on the Tensile, Thermal and Barrier Properties of Poly(Vinyl Alcohol) Nanocomposites, J. Nanomater., 2013 (2013) 1-9.

[75] W.J. Orts, J. Shey, S.H. Imam, G.M. Glenn, M.E. Guttman, J.-F. Revol, Application of Cellulose Microfibrils in Polymer Nanocomposites, J. of Polym. Environ., 13 (2005) 301-306.

[76] T. Zimmermann, E. Pöhler, T. Geiger, Cellulose Fibrils for Polymer Reinforcement, Adv. Eng. Mater., 6 (2004) 754-761.

[77] D. Roy, M. Semsarilar, J.T. Guthrie, S. Perrier, Cellulose modification by polymer grafting: a review, Chem. Soc. Rev., 38 (2009) 2046-2064.

[78] A. Isogai, T. Saito, H. Fukuzumi, TEMPO-oxidized cellulose nanofibers, Nanoscale, 3 (2011) 71-85.

[79] S. Eyley, W. Thielemans, Surface modification of cellulose nanocrystals, Nanoscale, 6 (2014) 7764-7779.

[80] S. Montanari, M. Roumani, L. Heux, M.R. Vignon, Topochemistry of Carboxylated Cellulose Nanocrystals Resulting from TEMPO-Mediated Oxidation, Macromolecules, 38 (2005) 1665-1671.

[81] J.L. Wu, C.G. Liu, X.L. Wang, Z.H. Huang, Preparation and characterization of nanoparticles based on histidine-hyaluronic acid conjugates as doxorubicin carriers, J. Mater. Sci. Mater. Med., 23 (2012) 1921-1929.

[82] P. Bulpitt, D. Aeschlimann, New strategy for chemical modification of hyaluronic acid: Preparation of functionalized derivatives and their use in the formation of novel biocompatible hydrogels, J. Biomed. Mater. Res., 47 (1999) 152-169.

[83] D. da Silva Perez, S. Montanari, M.R. Vignon, TEMPO-Mediated Oxidation of Cellulose III, Biomacromolecules, 4 (2003) 1417-1425.

[84] G. Kresse, J. Hafner, Ab initio molecular dynamics for liquid metals, Phys. Rev. B, 47 (1993) 558-561.

[85] S. Grimme, J. Antony, S. Ehrlich, H. Krieg, A consistent and accurate ab initio parametrization of density functional dispersion correction (DFT-D) for the 94 elements H-Pu, J. Chem. Phys., 132 (2010) 154104.

[86] P.E. Blöchl, Projector augmented-wave method, Phys. Rev. B, 50 (1994) 17953-17979.

[87] Y. Nishiyama, P. Langan, H. Chanzy, Crystal Structure and Hydrogen-Bonding System in Cellulose Iβ from Synchrotron X-ray and Neutron Fiber Diffraction, J. Am. Chem. Soc., 124 (2002) 9074-9082.

[88] J. Ireta, J. Neugebauer, M. Scheffler, On the Accuracy of DFT for Describing Hydrogen Bonds: Dependence on the Bond Directionality, J. Phys. Chem. A, 108 (2004) 5692-5698.

[89] D. Stillman, L. Krupp, Y.-H. La, Mesh-reinforced thin film composite membranes for forward osmosis applications: The structure–performance relationship, J. Membrane Sci., 468 (2014) 308-316.

[90] S.M. Mirkhalili, S.A. Mousavi, A.R. Saadat Abadi, M. Sadeghi, Preparation of mesh-reinforced cellulose acetate forward osmosis membrane with very low surface roughness, Korean J. Chem. Eng., 34 (2017) 3170-3177.

[91] P. Lu, Y.-L. Hsieh, Preparation and characterization of cellulose nanocrystals from rice straw, Carbohyd. Polym., 87 (2012) 564-573.

[92] A. Kardam, K.R. Raj, S. Srivastava, M.M. Srivastava, Nanocellulose fibers for biosorption of cadmium, nickel, and lead ions from aqueous solution, Clean Technol. Envir., 16 (2013) 385-393.

[93] X. Yu, S. Tong, M. Ge, L. Wu, J. Zuo, C. Cao, W. Song, Adsorption of heavy metal ions from aqueous solution by carboxylated cellulose nanocrystals, J. Environ. Sci., 25 (2013) 933-943.

[94] J. Glastrup, Degradation of polyethylene glycol. A study of the reaction mechanism in a model molecule: Tetraethylene glycol, Polym. Degrad. Stabil., 52 (1996) 217-222.

[95] T. Ohta, A. Tani, K. Kimbara, F. Kawai, A novel nicotinoprotein aldehyde dehydrogenase involved in polyethylene glycol degradation, Appl. Microbiol. Biot., 68 (2005) 639-646.

[96] A.W. Basit, J.M. Newton, M.D. Short, W.A. Waddington, P.J. Ell, L.F. Lacey, The Effect of Polyethylene Glycol 400 on Gastrointestinal Transit: Implications for the Formulation of Poorly-Water Soluble Drugs, Pharm. Res., 18 (2001) 1146-1150.

[97] R.G. Strickley, Solubilizing Excipients in Oral and Injectable Formulations, Pharm. Res., 21 (2004) 201-230.

[98] V. Dulong, G. Mocanu, L. Picton, D. Le Cerf, Amphiphilic and thermosensitive copolymers based on pullulan and Jeffamine®: Synthesis, characterization and physicochemical properties, Carbohyd. Polym., 87 (2012) 1522-1531.

[99] S. Belbekhouche, G. Ali, V. Dulong, L. Picton, D. Le Cerf, Synthesis and characterization of thermosensitive and pH-sensitive block copolymers based on polyetheramine and pullulan with different length, Carbohyd. Polym., 86 (2011) 304-312.

[100] F. Azzam, L. Heux, J.-L. Putaux, B. Jean, Preparation By Grafting Onto, Characterization, and Properties of Thermally Responsive Polymer-Decorated Cellulose Nanocrystals, Biomacromolecules, 11 (2010) 3652-3659.

[101] Y. Habibi, H. Chanzy, M.R. Vignon, TEMPO-mediated surface oxidation of cellulose whiskers, Cellulose, 13 (2006) 679-687.

[102] J. Araki, M. Wada, S. Kuga, Steric Stabilization of a Cellulose Microcrystal Suspension by Poly(ethylene glycol) Grafting, Langmuir, 17 (2001) 21-27.

[103] P. Lu, Y.-L. Hsieh, Preparation and properties of cellulose nanocrystals: Rods, spheres, and network, Carbohyd. Polym., 82 (2010) 329-336.

[104] Y. Boluk, C. Danumah, Analysis of cellulose nanocrystal rod lengths by dynamic light scattering and electron microscopy, J. Nanopart. Res., 16 (2013).

[105] P. Wang, M. Du, H. Zhu, S. Bao, T. Yang, M. Zou, Structure regulation of silica nanotubes and their adsorption behaviors for heavy metal ions: pH effect, kinetics, isotherms and mechanism, J. Hazard. Mater., 286 (2015) 533-544.

[106] M. de Martino, A. Chiarugi, Recent Advances in Pediatric Use of Oral Paracetamol in Fever and Pain Management, Pain Ther., 4 (2015) 149-168.

[107] K.C. Hyland, E.R.V. Dickenson, J.E. Drewes, C.P. Higgins, Sorption of ionized and neutral emerging trace organic compounds onto activated sludge from different wastewater treatment configurations, Water Res., 46 (2012) 1958-1968.

[108] F. Aloulou, S. Boufi, N. Belgacem, A. Gandini, Adsorption of cationic surfactants and subsequent adsolubilization of organic compounds onto cellulose fibers, Colloid Polym. Sci., 283 (2004) 344-350.

[109] P. Stenstad, M. Andresen, B.S. Tanem, P. Stenius, Chemical surface modifications of microfibrillated cellulose, Cellulose, 15 (2008) 35-45.

[110] P. Liu, P.F. Borrell, M. Božič, V. Kokol, K. Oksman, A.P. Mathew, Nanocelluloses and their phosphorylated derivatives for selective adsorption of Ag+, Cu2+ and Fe3+ from industrial effluents, J. Hazard. Mater., 294 (2015) 177-185.

[111] A. Kardam, K.R. Raj, S. Srivastava, M.M. Srivastava, Nanocellulose fibers for biosorption of cadmium, nickel, and lead ions from aqueous solution, Clean Technol. Envir., 16 (2014) 385-393.

[112] A. Sheikhi, S. Safari, H. Yang, T.G.M. van de Ven, Copper Removal Using Electrosterically Stabilized Nanocrystalline Cellulose, ACS Appl. Mater. Inter., 7 (2015) 11301-11308.

[113] T.S. Anirudhan, J.R. Deepa, J. Christa, Nanocellulose/nanobentonite composite anchored with multi-carboxyl functional groups as an adsorbent for the effective removal of Cobalt(II) from nuclear industry wastewater samples, J. Colloid Interf. Sci., 467 (2016) 307-320.

[114] X. He, K.B. Male, P.N. Nesterenko, D. Brabazon, B. Paull, J.H.T. Luong, Adsorption and Desorption of Methylene Blue on Porous Carbon Monoliths and Nanocrystalline Cellulose, ACS Appl. Mater. Inter., 5 (2013) 8796-8804.

[115] H. Qiao, Y. Zhou, F. Yu, E. Wang, Y. Min, Q. Huang, L. Pang, T. Ma, Effective removal of cationic dyes using carboxylate-functionalized cellulose nanocrystals, Chemosphere, 141 (2015) 297-303.

[116] A. Pei, N. Butchosa, L.A. Berglund, Q. Zhou, Surface quaternized cellulose nanofibrils with high water absorbency and adsorption capacity for anionic dyes, Soft Matter, 9 (2013) 2047-2055.

[117] K.J. De France, T. Hoare, E.D. Cranston, Review of Hydrogels and Aerogels Containing Nanocellulose, Chem. Mater., 29 (2017) 4609-4631.

[118] W. Maatar, S. Alila, S. Boufi, Cellulose based organogel as an adsorbent for dissolved organic compounds, Ind. Crop. Prod., 49 (2013) 33-42.

[119] A. Murray, B. Örmeci, Application of molecularly imprinted and non-imprinted polymers for removal of emerging contaminants in water and wastewater treatment: a review, Environ. Sci. Pollut. R., 19 (2012) 3820-3830.

[120] H.A. Karoyo, D.L. Wilson, Nano-Sized Cyclodextrin-Based Molecularly Imprinted Polymer Adsorbents for Perfluorinated Compounds—A Mini-Review, Nanomaterials, 5 (2015).

[121] C. Jae-Woo, B. Kyung-Youl, C. Kie-Yong, S. Natalia Valer¡¯yevna, L. Sang-Hyup, Amphiphilic Block Copolymer for adsorption of Organic Contaminants, Adv. Chem. Engineer. Sci., Vol.01No.02 (2011) 4.

[122] F. S. Bates, G. Fredrickson, Block Copolymers—Designer Soft Materials, 1999.

[123] M.B. Ahmed, J.L. Zhou, H.H. Ngo, M.A.H. Johir, L. Sun, M. Asadullah, D. Belhaj, Sorption of hydrophobic organic contaminants on functionalized biochar: Protagonist role of π-π electron-donor-acceptor interactions and hydrogen bonds, J. Hazard. Mater., 360 (2018) 270-278.

[124] Y. Xie, C.A.S. Hill, Z. Xiao, H. Militz, C. Mai, Silane coupling agents used for natural fiber/polymer composites: A review, Compos. Part A-Appl. S., 41 (2010) 806-819.

[125] Z. Zhang, G. Sèbe, D. Rentsch, T. Zimmermann, P. Tingaut, Ultralightweight and Flexible Silylated Nanocellulose Sponges for the Selective Removal of Oil from Water, Chem. Mater., 26 (2014) 2659-2668.

[126] H. Yousefi, T. Nishino, A. Shakeri, M. Faezipour, G. Ebrahimi, M. Kotera, Water-repellent all-cellulose nanocomposite using silane coupling treatment, J. Adhes. Sci. Technol., 27 (2013) 1324-1334.

[127] M.M. Bashar, H. Zhu, S. Yamamoto, M. Mitsuishi, Superhydrophobic surfaces with fluorinated cellulose nanofiber assemblies for oil–water separation, RSC Adv., 7 (2017) 37168-37174.

[128] S. Kalia, S. Boufi, A. Celli, S. Kango, Nanofibrillated cellulose: surface modification and potential applications, Colloid Polym. Sci., 292 (2014) 5-31.

[129] J. Herrera-Morales, K. Morales, D. Ramos, E.O. Ortiz-Quiles, J.M. López-Encarnación, E. Nicolau, Examining the Use of Nanocellulose Composites for the Sorption of Contaminants of Emerging Concern: An Experimental and Computational Study, ACS Omega, 2 (2017) 7714-7722.

[130] M. Castellano, A. Gandini, P. Fabbri, M.N. Belgacem, Modification of cellulose fibres with organosilanes: Under what conditions does coupling occur?, J. Colloid Interf. Sci., 273 (2004) 505-511.

[131] M.-C. Brochier Salon, M.N. Belgacem, Hydrolysis-Condensation Kinetics of Different Silane Coupling Agents, Phosphorus Sulfur, 186 (2011) 240-254.

[132] Y. Ren, X. Jiang, J. Yin, Copolymer of poly(4-vinylpyridine)-g-poly(ethylene oxide) respond sharply to temperature, pH and ionic strength, Euro. Polym. J., 44 (2008) 4108-4114.

[133] A.E. Reed, L.A. Curtiss, F. Weinhold, Intermolecular interactions from a natural bond orbital, donor-acceptor viewpoint, Chem. Rev., 88 (1988) 899-926.

[134] T.N. Tran, U. Paul, J.A. Heredia-Guerrero, I. Liakos, S. Marras, A. Scarpellini, F. Ayadi, A. Athanassiou, I.S. Bayer, Transparent and flexible amorphous cellulose-acrylic hybrids, Chem. Eng. J., 287 (2016) 196-204.

[135] Z. Souguir, A.-L. Dupont, K. Fatyeyeva, G. Mortha, H. Cheradame, S. Ipert, B. Lavédrine, Strengthening of degraded cellulosic material using a diamine alkylalkoxysilane, RSC Adv., 2 (2012) 7470-7478.

[136] J. Wang, L. Wan, S. Hao, J. Chen, Surface modification of diamond and its effect on the mechanical properties of diamond/epoxy composites, secm, 24 (2017) 271.

[137] M. Longhi, S.R. Kunsta, L.V.R. Beltrami, E.K. Kerstner, C.I. Silva Filho, V.H.V. Sarmento, C. Malfatti, Effect of Tetraethoxy-silane (TEOS) Amounts on the Corrosion Prevention Properties of Siloxane-PMMA Hybrid Coatings on Galvanized Steel Substrates, Mater. Res., 18 (2015) 1140-1155.

[138] Y. Xue, H. Xiao, Antibacterial/Antiviral Property and Mechanism of Dual-Functional Quaternized Pyridinium-type Copolymer, Polymers, 7 (2015).

[139] W. Li, Y. Wu, W. Liang, B. Li, S. Liu, Reduction of the Water Wettability of Cellulose Film through Controlled Heterogeneous Modification, ACS Appl. Mater. Inter., 6 (2014) 5726-5734.

[140] J.-J. Li, Y.-N. Zhou, Z.-H. Luo, Smart Fiber Membrane for pH-Induced Oil/Water Separation, ACS Appl. Mater. Inter., 7 (2015) 19643-19650.

[141] A. Gil, N. Taoufik, A.M. García, S.A. Korili, Comparative removal of emerging contaminants from aqueous solution by adsorption on an activated carbon, Environ. Technol., (2018) 1-14.

[142] M.B. Desta, Batch Sorption Experiments: Langmuir and Freundlich Isotherm Studies for the Adsorption of Textile Metal Ions onto Teff Straw (Eragrostis tef) Agricultural Waste, J. Thermodyn., 2013 (2013) 6.

[143] G.I. Mantanis, R.A. Young, R.M. Rowell, Swelling of compressed cellulose fiber webs in organic liquids, Cellulose, 2 (1995) 1-22.

[144] R.G. Candido, A.R. Gonçalves, Synthesis of cellulose acetate and carboxymethylcellulose from sugarcane straw, Carbohyd. Polym., 152 (2016) 679-686.

[145] A. Kaiser, W.J. Stark, R.N. Grass, Rapid Production of a Porous Cellulose Acetate Membrane for Water Filtration using Readily Available Chemicals, J. Chem. Educ., 94 (2017) 483-487.

[146] X. Jin, J. Shan, C. Wang, J. Wei, C.Y. Tang, Rejection of pharmaceuticals by forward osmosis membranes, Journal of Hazardous Materials, 227-228 (2012) 55-61.

[147] J. Xu, P. Li, M. Jiao, B. Shan, C. Gao, Effect of Molecular Configuration of Additives on the Membrane Structure and Water Transport Performance for Forward Osmosis, ACS Sustain. Chem. Eng., 4 (2016) 4433-4441.

[148] S.-W. Nam, C. Jung, H. Li, M. Yu, J.R.V. Flora, L.K. Boateng, N. Her, K.-D. Zoh, Y. Yoon, Adsorption characteristics of diclofenac and sulfamethoxazole to graphene oxide in aqueous solution, Chemosphere, 136 (2015) 20-26.

[149] J. Su, Q. Yang, J.F. Teo, T.-S. Chung, Cellulose acetate nanofiltration hollow fiber membranes for forward osmosis processes, J. Membrane Sci., 355 (2010) 36-44.

[150] S. Zhang, K.Y. Wang, T.-S. Chung, H. Chen, Y.C. Jean, G. Amy, Well-constructed cellulose acetate membranes for forward osmosis: Minimized internal concentration polarization with an ultra-thin selective layer, J. Membrane Sci., 360 (2010) 522-535.

[151] A. Idris, A.F. Ismail, M.Y. Noordin, S.J. Shilton, Optimization of cellulose acetate hollow fiber reverse osmosis membrane production using Taguchi method, J. Membrane Sci., 205 (2002) 223-237.

[152] A. Bódalo, J.-L. Gómez, E. Gómez, G. León, M. Tejera, Ammonium removal from aqueous solutions by reverse osmosis using cellulose acetate membranes, Desalination, 184 (2005) 149-155.

[153] X. Jin, J. Xu, X. Wang, Z. Xie, Z. Liu, B. Liang, D. Chen, G. Shen, Flexible TiO2/cellulose acetate hybrid film as a recyclable photocatalyst, RSC Adv., 4 (2014) 12640-12648.

[154] M. Hopp-Hirschler, U. Nieken, Modeling of pore formation in phase inversion processes: Model and numerical results, J. Membrane Sci., 564 (2018) 820-831.

[155] J. Heo, L.K. Boateng, J.R.V. Flora, H. Lee, N. Her, Y.-G. Park, Y. Yoon, Comparison of flux behavior and synthetic organic compound removal by forward osmosis and reverse osmosis membranes, J. Membrane Sci., 443 (2013) 69-82.

[156] V.F. Roche, The chemically elegant proton pump inhibitors, Am J Pharm Educ, 70 (2006) 101-101.

[157] L. Zhang, Y. Wang, S. Jin, Q. Lu, J. Ji, Adsorption isotherm, kinetic and mechanism of expanded graphite for sulfadiazine antibiotics removal from aqueous solutions, Environ. Technol., 38 (2017) 2629-2638.

[158] Y.S. Ho, G. McKay, Pseudo-second order model for sorption processes, Process Biochem., 34 (1999) 451-465.

[159] S. Azizian, Kinetic models of sorption: a theoretical analysis, J. Colloid Interf. Sci., 276 (2004) 47-52.

[160] Y.-S. Ho, Review of second-order models for adsorption systems, J. Hazard. Mater., 136 (2006) 681-689.

[161] J.-M. Chern, Y.-W. Chien, Competitive adsorption of benzoic acid and p-nitrophenol onto activated carbon: isotherm and breakthrough curves, Water Res., 37 (2003) 2347-2356.

[162] J.-M. Chern, Y.-W. Chien, Adsorption of nitrophenol onto activated carbon: isotherms and breakthrough curves, Water Res., 36 (2002) 647-655.

[163] G.R. Guillen, Y. Pan, M. Li, E.M.V. Hoek, Preparation and Characterization of Membranes Formed by Nonsolvent Induced Phase Separation: A Review, Ind. Eng. Chem. Res., 50 (2011) 3798-3817.

# APPENDIX

**Table S1**. Isotherm plots of for the adsorption of CECs with NC and Oxidized NC at different pHs.

| Adsorbate | Acetaminophen | Sulfamethoxazole | DEET |
|---|---|---|---|
| NC | 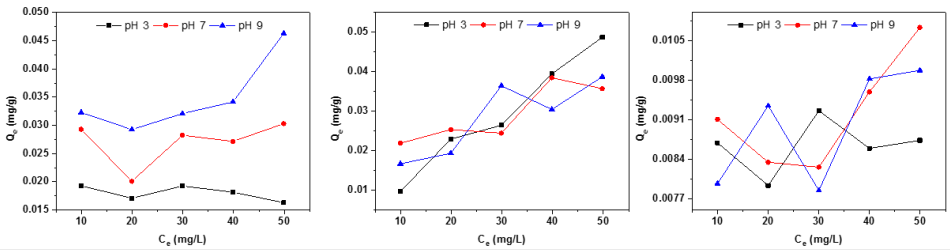 | | |
| Oxidized NC | 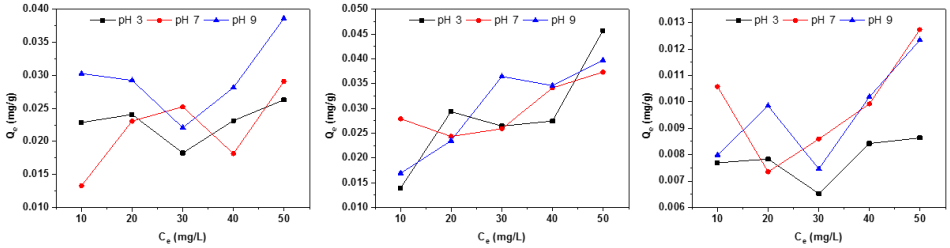 | | |

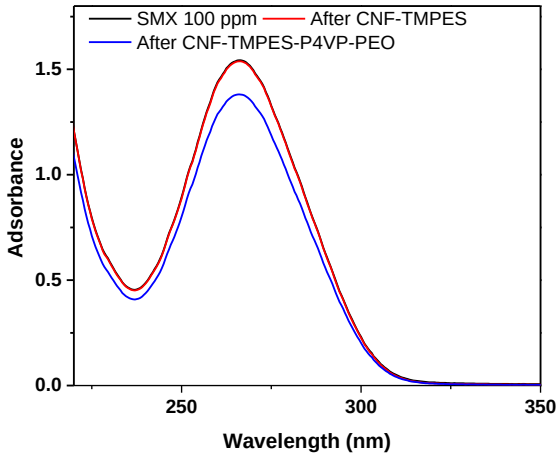


**Figure S1.** UV-Vis spectra of SMX, And SMX after 24 h contact time with TMPES-modified CNFs films with and without P4VP-PEO.

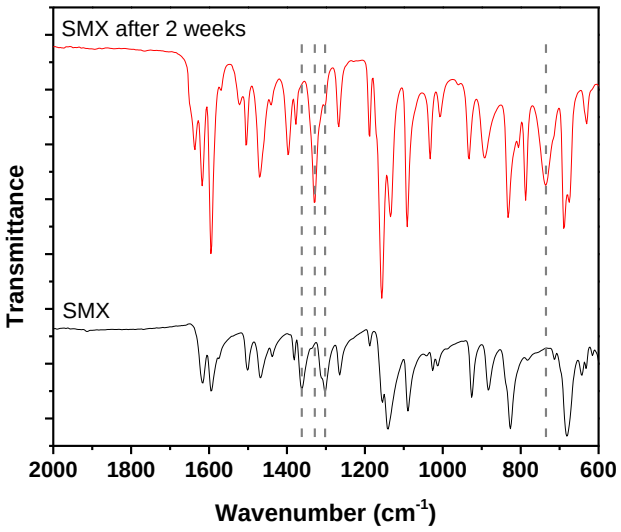


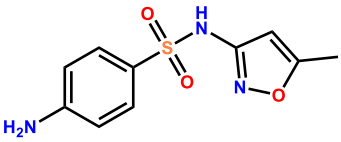


**Figure S2.** Freshly prepared 200 ppm SMX solution (top, left). 200 ppm SMX solution after 2 weeks (top, right). FTIR spectra of SMX powder from the bottle and lyophilized 2 weeks 200 ppm SMX solution.